Event-triggered boundary control of the linearized Fitzhugh-Nagumo equation

Víctor Hernández-Santamaría, Subrata Majumdar, Luz de Teresa

Event-triggered boundary control of the linearized FitzHugh-Nagumo equation*

Víctor Hernández-Santamaría[a,1], Subrata Majumdar[a,2], Luz de Teresa[a,*]

[a]*Instituto de Matemáticas, Universidad Nacional Autónoma de México, Circuito Exterior C.U., CDMX, 04510, Mexico*

Abstract

In this paper, we address the exponential stabilization of the linearized FitzHugh-Nagumo system using an event-triggered boundary control strategy. Employing the backstepping method, we derive a feedback control law that updates based on specific triggering rules while ensuring the exponential stability of the closed-loop system. We establish the well-posedness of the system and analyze its input-to-state stability in relation to the deviations introduced by the event-triggered control. Numerical simulations demonstrate the effectiveness of this approach, showing that it stabilizes the system with fewer control updates compared to continuous feedback strategies while maintaining similar stabilization performance.

Keywords:
Coupled parabolic-ODE system, stabilization by feedback, critical decay rate, Lyapunov function, Volterra transformation
2020 MSC: 93C65, 93C20, 93B52, 93D15, 35M32

1. Introduction

1.1. Motivation

In control systems, particularly when implemented on digital platforms, a key challenge is balancing performance with resource usage. Traditional digital control schemes, such as sampled-data control, typically rely on periodic updates of the control signal. However, this can lead to unnecessary computational effort, especially when the system state evolves slowly. This issue is even more critical in networked control systems, where excessive communication can exhaust available resources (see, for example, [20] for a more detailed introduction in the finite-dimensional case, and [23, 24] for applications in the parabolic setting).

Event-triggered control has emerged as an effective alternative, performing updates only when a predefined condition (based on the system state) is fulfilled. This approach allows the system to remain stable while minimizing control updates and preserving resources. The approach has shown promising results in finite-dimensional systems modelled by ordinary differential equations (ODEs) [45, 36] and, more recently, in systems described by partial differential equations (PDEs), see e.g., [2, 12, 16, 21, 27, 40, 3, 49, 44, 11, 28, 38, 39, 10, 37].

In the context of PDEs, the most common stabilization results rely on controlling from the boundary of the equation. The backstepping technique (see the seminal work [29]) offers a systematic approach for designing stabilizing feedback laws applicable to a wide range of systems. One of its key advantages is that this method is robust and adaptable across various frameworks, having been successfully applied to numerous equations and models while ensuring global stability. We refer to the non-exhaustive list [8, 17, 7, 1, 31, 9, 19, 34] for recent progress and works in this direction. We also refer to the very nice survey [46] and its references for a broader perspective on current trends in the backstepping technique.

Building on this framework, we consider the application of event-triggered control to a system known as the FitzHugh-Nagumo model. We employ the backstepping feedback as a starting point and apply the event-triggered control strategy to a linearized version of the model. As established in prior work (see [5]), this linearization possesses specific stabilization properties, most notably the restriction that stabilization can only be achieved for decay parameters determined by the system's coefficients rather than arbitrary values. We extend this analysis to the event-triggered setting, demonstrating that the system remains stable and that the stabilization rate can be made arbitrarily close to that of the continuous control case.

1.2. State of the art

Event-triggered control for partial differential equations has gained significant attention in recent years, resulting in a vast and rich body of literature across various classes of PDEs. Let us provide an overview of the most relevant areas and highlight key works related to these topics.

For hyperbolic PDEs, the work in [14] introduces an output feedback event-triggered boundary controller for one-dimensional linear hyperbolic systems of conservation laws,

*This work has received support from Project A1-S-17475 of CONAHCYT, Mexico.

*Corresponding author.
Email addresses: victor.santamaria@im.unam.mx (Víctor Hernández-Santamaría), subrata.majumdar@im.unam.mx (Subrata Majumdar), ldeteresa@im.unam.mx (Luz de Teresa)

[1]V. Hernández-Santamaría is supported by the program "Estancias Posdoctorales por México para la Formación y Consolidación de las y los Investigadores por México" of CONAHCYT (Mexico). He also received support from Project CBF2023-2024-116 of CONAHCYT and by UNAM-DGAPA-PAPIIT grants IN117525, IA100324 and IN102925 (Mexico).

[2]S. Majumdar is supported by the UNAM Postdoctoral Program (POSDOC).

utilizing Lyapunov techniques (see also [43] for the case of a 2×2 hyperbolic system with periodic updates). By employing the backstepping method, the works [12, 15] develop dynamic triggering conditions for event-triggered boundary controllers aimed at stabilizing coupled 2×2 linear hyperbolic systems, using full-state feedback and output feedback, respectively. Further advancements of this approach can be found in [48, 49], with [49] specifically presenting an event-triggered adaptive control strategy for coupled hyperbolic PDEs. These backstepping-based event-triggered control techniques have also been applied to practical systems, such as load-moving cable systems [47] and traffic flow regulation on interconnected roads [13].

Regarding parabolic PDEs, [42] introduces a decentralized event-triggered control approach to minimize the number of transmitted measurements. Meanwhile, [25] employs modal decomposition to design a sampled-data and observer-based event-triggered boundary control scheme for one-dimensional reaction-diffusion systems with time-varying input delays. This approach features a novel switching-based dynamic triggering condition that depends on the estimated state's finite modes, combined with time regularization to prevent the Zeno phenomenon. Alternatively, using Input-to-State Stability (ISS) properties for PDEs and small-gain arguments, the work [16] proposes a backstepping-based event-triggering control strategy for a one-dimensional reaction-diffusion system with constant parameters and Dirichlet boundary actuation. Additionally, [40] introduces an observer-based event-triggered backstepping boundary control under Robin boundary actuation. This strategy incorporates a dynamic triggering condition that ensures a minimum dwell time, thereby preventing the Zeno phenomenon. Another approach to event-triggering based control has been studied in [22], where the authors applied a gain scheduling type strategy for a reaction-diffusion system with time and space varying reaction coefficients. More recent advances can be found, for instance, in [39], where the notion of performance is incorporated into the event-triggering strategy. This means that the expected decay of the Lyapunov functional (and, consequently, the system's stability) must be ensured while keeping the system's operation within a prescribed threshold (see also [50] for a traffic-flow model).

Furthermore, [49] extends the findings of [40] by proposing an adaptive event-triggered boundary control scheme for a cascade parabolic PDE-ODE system with uncertain parameters. Expanding on these ideas, [37] explores applications to the Stefan problem. It is worth mentioning that the event-triggered control methods have also been studied in other classes of PDEs, including reaction-diffusion PDEs with input delay, see [28]. This problem essentially reduces to stability issues for a coupled parabolic-transport (hyperbolic PDE-ODE) system. Other notable contributions include [21], which examines event-triggered control for the nonlinear Korteweg–de Vries (KdV) equation under averaged measurements, [27] for the damped linear wave equation, and [26] for the damped linear Schrödinger equation, among others.

In this paper, we explore the event-triggering control strategy for a backstepping-based feedback controller applied to the linearized FitzHugh-Nagumo equation. Our stability analysis relies on Input-to-State Stability and small-gain principles, following the approach in [16] for a scalar parabolic equation. The main difficulty lies in extending the analysis of that work to a coupled parabolic-ODE system, where the ODE component also depends on the spatial variable. This makes the ODE component infinite-dimensional, in contrast to the coupled PDE-ODE system studied in [49]. This feature introduces an accumulating spectral branch, which complicates the analysis and prevents achieving an arbitrary (prescribed) exponential decay rate. Here, we establish the existence of a uniform minimal dwell time—independent of the initial conditions—between consecutive triggering instants, thereby preventing the Zeno phenomenon. Consequently, we ensure the well-posedness of the closed-loop system, guaranteeing the existence and uniqueness of solutions, as well as its global exponential stability.

1.3. Setting of the problem

Let us consider the following nonlinear coupled ODE-PDE reaction-diffusion system in the interval $(0,1)$ with non-monotone non-linearity $I_{\text{ion}}(\cdot,\cdot)$ of FitzHugh-Nagumo type

$$\begin{cases} \partial_t v = \partial_x^2 v + I_{\text{ion}}(v,w) & \text{in } (0,\infty)\times(0,1),\\ \partial_t w = \gamma v - \delta w & \text{in } (0,\infty)\times(0,1),\\ v(t,0) = 0, \;\; v(t,1) = q(t) & \text{in } (0,\infty),\\ v(0,x) = v_0(x), \;\; w(0,x) = w_0(x) & \text{in } (0,1). \end{cases} \tag{1}$$

In (1), $v = v(x,t)$ and $w = w(x,t)$ are the state variables while $q \in L^2(0,\infty)$ is a boundary control. The nonlinearity is of the form:

$$I_{\text{ion}}(v,w) = -v(v-1)(v-a) - \rho w.$$

Here, the system parameters are $a \in (0,1)$, and γ, δ, and ρ are positive constants.

We refer the reader to the review article [18] for a comprehensive study of this mathematical model in neurobiology. This model describes the conduction of electrical impulses in a nerve axon (see also [41]) and is also known in cardiac electrophysiology as the monodomain equations (see [35] for more details).

In this paper, we are interested in studying the exponential stabilization by means of an event-triggered control of the following linearized version (around the origin) of (1)

$$\begin{cases} \partial_t v = \partial_x^2 v - av - \rho w & \text{in } (0,\infty)\times(0,1),\\ \partial_t w = \gamma v - \delta w & \text{in } (0,\infty)\times(0,1),\\ v(t,0) = 0, \;\; v(t,1) = q(t) & \text{in } (0,\infty),\\ v(0,x) = v_0(x) \quad w(0,x) = w_0(x) & \text{in } (0,1). \end{cases} \tag{2}$$

We begin by recalling the notion of exponential stabilization by feedback control.

Definition 1.1. Let $(v_0, w_0) \in L^2(0,1)\times L^2(0,1)$. The system (2) is called exponential stabilizable by feedback control in the space $L^2(0,1)\times L^2(0,1)$ with a decay rate $\omega > 0$, if there exists a bounded linear map $\Pi : L^2(0,1)\times L^2(0,1) \to \mathbb{R}$ such that, the

solution (v, w) of (2) with control of the form $q(t) = \Pi(v, w)(t, \cdot)$ satisfies

$$\|v(t)\|_{L^2(0,1)} + \|w(t)\|_{L^2(0,1)} \leq Ce^{-\omega t}\left(\|v_0\|_{L^2(0,1)} + \|w_0\|_{L^2(0,1)}\right),$$

for all $t > 0$, for some positive constant C independent of u_0 and w_0.

It is well-known that the system (2) is not exponentially stabilizable in the sense of Definition 1.1 with a exponential decay $e^{-\omega t}$ if $\omega > \delta$ (see [5, Corollary 3.13]). This limitation arises due to the presence of the ODE component in (2), which acts as a memory term, preventing any improvement in the decay rate beyond the critical value δ. See [6], [4], and [30] for this kind of obstruction in related control problems.

Despite the obstruction to exponential stabilization when $\omega > \delta$, feedback control still plays a role in enhancing the system's stability with decay rate $\omega \leq \delta$. By direct computations, it can be checked that if $q = 0$, system (2) is exponentially stable with decay rate $\omega = \min\{a, \delta\}$. On the other hand, it has been proved in [5] that using the method of backstepping, we can go up to the exponential decay $e^{-\omega t}$ for any $\omega \leq \delta$. According to these facts, if $\delta < a$, system (2) with $q = 0$ already exhibits the expected exponential stability. Consequently, the case $\delta > a$ is the most relevant for the design of the feedback control law because in this case the exponential decay is e^{-at}, which we know that can be improved by feedback controls. This motivates us to study the event-triggering control strategy and investigate whether the best possible decay rate can be achieved.

The stabilization result in [5] is established by the action of an explicit feedback control law of the form

$$q(t) = v(t, 1) = \int_0^1 k(1, y)v(t, y)\mathrm{d}y, \quad t > 0, \tag{3}$$

where k is a suitable kernel (see eq. (6) in Section 2). In this paper, employing an event-triggering approach, we replace the continuous control (3) by

$$q_d(t) = v(t, 1) = \int_0^1 k(1, y)v(t_j, y)\mathrm{d}y,$$

for all $t \in [t_j, t_{j+1})$, $j \in \mathbb{N}$, where $\{t_j\}_j$ is a sequence of triggering times obeying a well-prescribed rule (see Definition 4.1 below). The price to pay for applying this piecewise-constant control is that we are unable to achieve the critical decay rate δ, but only the exponential rate

$$e^{-\omega t} \quad \text{where} \quad \omega = \delta - \epsilon \quad \forall \epsilon \in (0, \delta). \tag{4}$$

See Theorem 4.8 below.

1.4. Outline of the paper

The rest of the paper is organized as follows. In Section 2, we describe a preliminary structure of the backstepping approach along with the event-triggering control strategy. Section 3 contains well-posedness results for the event-triggered control system. Section 4 is devoted to the description of the event-triggering rule, the avoidance of the occurrence of the Zeno solution and the main result (Theorem 4.8) regarding the exponential stabilization of the linearized FHN system. Finally, in Section 5, we conclude the paper by introducing some numerics which illustrate the result of the paper.

2. Brief description on the structure of Backstepping under the Event-triggered strategy

Our main goal is to investigate the exponential stabilizability of the closed-loop linear FHN system (2) with an event-triggered approach. This method involves stabilization based on events by sampling the feedback control law (3) for the continuous-time backstepping case at specific time instants, which form an increasing sequence $\{t_j\}_{j\in\mathbb{N}}$, along with $t_0 = 0$. These time instants will be characterized later through a triggering rule. Between two consecutive time instants, the control value remains constant and is only updated when a state-dependent condition is satisfied.

In this context, we will use the boundary control of the form

$$v(t, 1) = q_d(t) = \int_0^1 k(1, y)v(t_j, y)\mathrm{d}y, \tag{5}$$

for all $t \in [t_j, t_{j+1})$, $j \in \mathbb{N}$, where k satisfies the following wave equation in the triangle $\mathcal{T} = \{(x, y) \in [0, 1] \times [0, 1] : 0 \leq y \leq x \leq 1\}$

$$\begin{cases} \partial_x^2 k(x, y) - \partial_y^2 k(x, y) - (\lambda - a)k(x, y) = 0 & 0 < y < x < 1, \\ 2\dfrac{\mathrm{d}}{\mathrm{d}x}k(x, x) + (\lambda - a) = 0 & 0 \leq x \leq 1, \\ k(x, 0) = 0, & 0 \leq x \leq 1, \end{cases} \tag{6}$$

where λ is a positive constant. Thanks to Lemma 2.2 of [32] and Lemma 4.4 of [33], we see that the equation (6) has a unique C^2 solution. Furthermore, we can write the solution k in the following series expansion

$$k(x, y) = -\sum_{n=0}^{\infty}\left(\frac{\lambda - a}{4}\right)^{n+1}\frac{2y(x^2 - y^2)^n}{(n!)^2\,(n + 1)},$$

and thanks to [29, Chapter 4], we also have the following representation

$$k(x, y) = (a - \lambda)y\frac{\mathcal{I}_1\left(\sqrt{(a - \lambda)(y^2 - x^2)}\right)}{\sqrt{(a - \lambda)(y^2 - x^2)}}, \tag{7}$$

where $\mathcal{I}_1$ is the Bessel function given by $\mathcal{I}_1 = \sum_{n=0}^{\infty}\frac{(\frac{x}{2})^{1+2n}}{n!(n+1)!}$.

Note that, the expression of the control q_d in (5) can be written in the following fashion

$$q_d(t) = \underbrace{\int_0^1 k(1, y)v(t, y)\mathrm{d}y}_{q(t)} + d(t), \tag{8}$$

where $d(t)$ is the difference between the event triggering control and the continuous-time backstepping control at $t \in [t_j, t_{j+1})$

$$d(t) = \int_0^1 k(1,y)v(t_j,y)\mathrm{d}y - \int_0^1 k(1,y)v(t,y)\mathrm{d}y. \tag{9}$$

Let us formulate the concerned system with an event-triggered control strategy $\forall j \in \mathbb{N}$

$$\begin{cases} \partial_t v = \partial_x^2 v - av - \rho w & \text{in } (t_j, t_{j+1}) \times (0,1), \\ \partial_t w = \gamma v - \delta w & \text{in } (t_j, t_{j+1}) \times (0,1), \\ v(t,0) = 0, & \text{in } (t_j, t_{j+1}), \\ v(t,1) = \int_0^1 k(1,y)v(t_j,y)\mathrm{d}y & \text{in } (t_j, t_{j+1}), \end{cases} \tag{10}$$

and initial conditions $v(0,x) = v_0(x)$, $w(0,x) = w_0(x)$ in $(0,1)$. Next, we employ the well-known backstepping method for the event-triggered boundary control system (10). For that, let us introduce the Volterra integral transformation of the second kind $\Pi : L^2(0,1) \to L^2(0,1)$ defined by

$$(\Pi\sigma)(x) = \sigma(x) - \int_0^x k(x,y)\sigma(y)\mathrm{d}y, \quad x \in [0,1],\ \sigma \in L^2(0,1), \tag{11}$$

where the kernel function k is the solution of equation (6). Note that $\Pi : L^2(0,1) \to L^2(0,1)$ and $\Pi^{-1} : L^2(0,1) \to L^2(0,1)$ are linear bounded operators (see Lemma 2.4 in [32]). The inverse of the transformation (11) is given by

$$(\Pi^{-1}\hat{\sigma})(x) = \hat{\sigma}(x) + \int_0^x l(x,y)\hat{\sigma}(y)\mathrm{d}y, \quad x \in [0,1], \tag{12}$$

where l is the solution of the following equation

$$\begin{cases} \partial_x^2 l(x,y) - \partial_y^2 l(x,y) + (\lambda - a)l(x,y) = 0 & 0 < y < x < 1, \\ 2\dfrac{\mathrm{d}}{\mathrm{d}x} l(x,x) + (\lambda - a) = 0 & 0 \le x \le 1, \\ l(x,0) = 0 & 0 \le x \le 1. \end{cases} \tag{13}$$

Using the transformation (11), let us define

$$\begin{cases} u(t,\cdot) = \Pi v(t,\cdot), \\ z(t,\cdot) = \Pi w(t,\cdot). \end{cases} \tag{14}$$

Next, one can show that the system (10) can be transformed to the following target system

$$\begin{cases} \partial_t u - \partial_x^2 u + \lambda u + \rho z = 0 & \text{in } (t_j, t_{j+1}) \times (0,1), \\ \partial_t z = \gamma u - \delta z & \text{in } (t_j, t_{j+1}) \times (0,1), \\ u(t,0) = 0, \quad u(t,1) = d(t) & \text{in } (t_j, t_{j+1}), \\ u(0,x) = u_0(x), \quad z(x,0) = z_0(x) & \text{in } (0,1). \end{cases} \tag{15}$$

where $\lambda > 0$ is called the damping parameter, to be chosen as sufficiently large (see (41) and Remark 4.7 for details), (u,z), d are given by (14) and (9), respectively and u_0, z_0 are the following

$$\begin{cases} u_0(x) = \Pi v_0 = v_0(x) - \int_0^x k(x,y)v_0(y)\mathrm{d}y, \\ z_0(x) = \Pi w_0 = w_0(x) - \int_0^x k(x,y)w_0(y)\mathrm{d}y. \end{cases}$$

In order to establish the exponential stabilizability of the system (10), we first prove that the target system (15) is exponentially stable and then, thanks to the invertibility of the Volterra transformation (11), we get the stabilization result for (10). It is worth mentioning that, in the continuous backstepping case instead of the target system (15) with nonhomogeneous boundary data at the right Dirichlet end, we have a similar system with homogeneous boundary data, and thus one can obtain the exponential stability with critical exponential decay rate up to $e^{-\delta t}$, see [5] for more details. For the event-triggering case, due to the presence of a nonhomogeneous boundary data $u(t,1) = d(t)$ in the target system (15), we get the exponential stability of the system (15) with a decay rate $\omega < \delta$. This fact essentially implies the same result for the original event-triggered system (10).

3. Well-posedness result

Through this section, let $\{t_j\}_{j\in J}$, $J \subset \mathbb{N}$, be a strictly increasing sequence of times. We start by introducing the maximal time T under which the system (10) possess a solution

$$T := \begin{cases} \infty, & \text{if } \{t_j\} \text{ is a finite sequence}, \\ \limsup\limits_{j\to\infty} t_j & \text{otherwise.} \end{cases} \tag{16}$$

Theorem 3.1. *For every* $\big(v(t_j), w(t_j)\big) \in L^2(0,1) \times L^2(0,1)$, *system* (10) *possess a unique solution* $(v,w) \in C^0([t_j, t_{j+1}]; L^2(0,1)\times L^2(0,1)) \cap L^2(t_j, t_{j+1}; H^1(0,1)\times L^2(0,1))$.

Proof. We prove this result by establishing a similar result for a system with homogeneous boundary conditions and then performing a change of variable, we conclude the result for the main system (10). Note that the boundary data for the right end (at $x = 1$) of v is constant in the interval (t_j, t_{j+1}) and we denote $\bar{q} = q_d$. Next, we consider the following system

$$\begin{cases} \partial_t \bar{v} = \partial_x^2 \bar{v} - a\bar{v} - \rho\bar{w} - \bar{q}\left(a + \frac{\rho\gamma}{\delta}\right)x & \text{in } (t_j, t_{j+1}) \times (0,1), \\ \partial_t \bar{w} = \gamma\bar{v} - \delta\bar{w} & \text{in } (t_j, t_{j+1}) \times (0,1), \\ \bar{v}(t,0) = 0, \ \bar{v}(t,1) = 0 & \text{in } (t_j, t_{j+1}). \end{cases} \tag{17}$$

As it is given that $\big(v(t_j), w(t_j)\big) \in L^2(0,1) \times L^2(0,1)$, thanks to [5, Lemma A.1], the solution of (17) lies in the space $C^0([t_j, t_{j+1}]; L^2(0,1)\times L^2(0,1)) \cap L^2(t_j, t_{j+1}; H^1(0,1)\times L^2(0,1))$. Next taking, $v = \bar{v} + \bar{q}x$, $w = \bar{w} + \frac{\bar{q}\gamma}{\delta}x$, $\bar{q} = \int_0^1 k(1,y)v(t_j,y)dy$, one can show that (v,w) satisfies (10) and

$$(v,w) \in C^0([t_j, t_{j+1}]; L^2(0,1) \times L^2(0,1)) \cap L^2(t_j, t_{j+1}; H^1(0,1) \times L^2(0,1)).$$

This ends the proof. □

The above well-posedness result allows us to construct a solution (v,w) for the system (10) in the time interval $[0,T)$.

Corollary 3.2. *Let* $(v_0, w_0) \in L^2(0,1) \times L^2(0,1)$. *Then there exists unique mapping* (v,w) *such that* $(v,w) \in C^0\big([0,T); L^2(0,1) \times L^2(0,1)\big)$ *with* $v(t) \in H^1(0,1)$, *for a.e.* $t \in (0,T)$ *and* (v,w) *satisfies* (10) *in* (t_j, t_{j+1}), $\forall j \in \mathbb{N}$.

Proof. First let us consider that $(v_0, w_0) \in L^2(0,1) \times L^2(0,1)$. Then using Theorem 3.1, we get the existence of unique solution of (10) in $(t_0, t_1) = (0, t_1)$ denoted by (v^0, w^0) and we have $(v^0, w^0) \in C^0([0, t_1]; L^2(0,1) \times L^2(0,1))$. with $v^0(t) \in H^1(0,1)$ for a.e. $t \in (0, t_1]$. Note that we get $(v^0(t_1), w^0(t_1)) \in L^2(0,1) \times L^2(0,1)$. Thus we start the system in the next interval (t_1, t_2) with taking $(v^0(t_1), w^0(t_1))$ as the initial data and so on. That is, at each step, we have the following system for $(j \geq 1)$

$$\begin{cases} \partial_t v^j = \partial_x^2 v^j - a v^j - \rho w^j & \text{in } (t_j, t_{j+1}) \times (0,1), \\ \partial_t w^j = \gamma v^j - \delta w^j & \text{in } (t_j, t_{j+1}) \times (0,1), \\ v^j(t,0) = 0, & \text{in } (t_j, t_{j+1}), \\ v^j(t,1) = \int_0^1 k(1,y) v^j(t_j, y) \mathrm{d}y & \text{in } (t_j, t_{j+1}), \\ v^j(t_j, x) = v^{j-1}(t_j, x) & \text{in } (0,1), \\ w^j(t_j, x) = w^{j-1}(t_j, x) & \text{in } (0,1), \end{cases} \tag{18}$$

and we get the existence of unique solution $(v^j, w^j) \in C^0([t_j, t_{j+1}]; L^2(0,1) \times L^2(0,1))$ with $\left(v^j(t), w^j(t)\right) \in H^1(0,1) \times L^2(0,1)$, for a.e $t \in (t_j, t_{j+1}]$. With this step-by-step construction, we finally have the solution $(v, w) = (v^j, w^j)$ in $[t_j, t_{j+1}]$ with the desired regularity. □

4. Exponential stabilizability

The main goal of this section is to present the event-triggered boundary control and its primary outcomes: avoidance of the Zeno phenomenon and the exponential stability of the event-triggered controlled system. The event-triggered boundary control discussed in this paper includes a triggering condition, which determines the moments when the controller needs to be updated, and a backstepping-based boundary feedback law, applied at the right end of the Dirichlet boundary for the parabolic component. The proposed event-triggering condition is based on the evolution of the L^2 norms of the states of both the parabolic and the ODE components.

4.1. Event-triggered rule

Let us denote $V(t) = \|v(t)\|_{L^2(0,1)} + \|w(t)\|_{L^2(0,1)}$, where (v, w) is the solution of the equation (10).

Definition 4.1. Let $\beta > 0$ be a parameter that will be chosen later. Let us recall the kernel k defined in (6) and the control d in (9). Let us define the following set:

$$E(t_j) := \Big\{ t > 0 : t > t_j \quad \text{and} \\ |d(t)| > \beta \|k(1,\cdot)\|_{L^2(0,1)} V(t) + \beta \|k(1,\cdot)\|_{L^2(0,1)} V(t_j) \Big\}. \tag{19}$$

The event-triggered boundary control is defined by considering the following components:

1. (The event-trigger) The times of the events $t_j \geq 0$ with $t_0 = 0$ form a finite or countable set of times which is determined by the following rules for some $j \in \mathbb{N}$:

   a) if $E(t_j) = \emptyset$ then the set of the times of the events is $\{t_0, ..., t_j\}$.

   b) if $E(t_j) \neq \emptyset$, then the next event time is given by:

   $$t_{j+1} = \inf E(t_j) \tag{20}$$

2. (The control action) The boundary feedback law,

   $$q_d(t) = \int_0^1 k(1,y) v(t_j, y) \mathrm{d}y, \quad \forall t \in [t_j, t_{j+1}). \tag{21}$$

4.2. Avoidance of Zeno behavior

In this section, we will prove that the so-called Zeno phenomenon, which refers to an infinite number of triggers in a finite time interval, is avoided by ensuring minimal dwell time between two triggering instances. Let us first present the following intermediate result before moving to the finding of the existence of the minimal dwell time.

Lemma 4.2. *For the closed-loop system (10), the following estimate holds, for all $t \in [t_j, t_{j+1}]$, $j \in \mathbb{N}$:*

$$\sup_{t_j \leq s \leq t_{j+1}} \left(\|v(s)\|_{L^2(0,1)} + \|w(s)\|_{L^2(0,1)} \right) \\ \leq M_j \left(\|v(t_j)\|_{L^2(0,1)} + \|w(t_j)\|_{L^2(0,1)} \right) \tag{22}$$

where $M_j = \sqrt{2} e^{\frac{c}{2}(t_{j+1} - t_j)} \left(1 + \|k(1,\cdot)\|_{L^2(0,1)} + \frac{\|k(1,\cdot)\|_{L^2(0,1)}}{\sqrt{c}} \right) + \|k(1,\cdot)\|_{L^2(0,1)}$ *and c is a positive constant that depends on the system parameters.*

Proof. Let us first introduce the following change of variables

$$\begin{cases} \tilde{v}(t,x) = v(t,x) - x q_d(t), \\ \tilde{w}(t,x) = w(t,x). \end{cases} \tag{23}$$

It is easy to check that $(\tilde{v}, \tilde{w})$ satisfies the following PDE for all $t \in (t_j, t_{j+1})$, $j \in \mathbb{N}$,

$$\begin{cases} \tilde{v}_t = \partial_x^2 \tilde{v} - a\tilde{v} - \rho \tilde{w} - a x q_d & \text{in } (t_j, t_{j+1}) \times (0,1), \\ \tilde{w}_t = \gamma \tilde{v} - \delta \tilde{w} + \gamma x q_d(t) & \text{in } (t_j, t_{j+1}) \times (0,1), \\ \tilde{v}(t,0) = 0, \ \tilde{v}(t,1) = 0 & \text{in } (t_j, t_{j+1}). \end{cases} \tag{24}$$

Next, by considering the function

$$W(t) := \frac{1}{2} \left(\|\tilde{v}(t)\|^2_{L^2(0,1)} + \|\tilde{w}(t)\|^2_{L^2(0,1)} \right)$$

and taking its time derivative along the solutions of (24) and using Cauchy-Schwarz inequality for the coupling terms, we obtain, for $t \in (t_j, t_{j+1})$:

$$\dot{W}(t) \leq - \|\partial_x \tilde{v}(t)\|^2_{L^2(0,1)} - a\|\tilde{v}(t)\|^2_{L^2(0,1)} - \delta \|\tilde{w}(t)\|^2_{L^2(0,1)} \\ + (\rho + \gamma) W(t) + q_d \int_0^1 (\gamma x \tilde{w} - a x \tilde{v}) \mathrm{d}x.$$

In addition, using the Young's inequality on the last term along with the Cauchy-Schwarz inequality, we get

$$\dot{W}(t) \leq c_1 W(t) + \frac{1}{2} q_d^2 + c_2 W(t),$$

where c_1, c_2 are two positive constants. Then, for $t \in (t_j, t_{j+1})$:

$$\dot{W}(t) \leq cW(t) + \frac{1}{2}q_d^2,$$

where c is a positive constant. Thanks to the Gronwall's inequality on an interval $[p, r]$ where $p > t_j$ and $r < t_{j+1}$, one gets, for all $t \in [p, r]$

$$W(t) \leq e^{c(t-p)}\left(W(p) + \frac{1}{2c}q_d^2\right).$$

Due to the continuity of $W(t)$ on $[t_j, t_{j+1}]$ and the fact that p, r are arbitrary, we can conclude that

$$W(t) \leq e^{c(t_{j+1}-t_j)}\left(W(t_j) + \frac{1}{2c}q_d^2\right) \tag{25}$$

for all $t \in [t_j, t_{j+1}]$. Then, applying Cauchy-Schwarz inequality, we have that

$$|q_d| \leq \|k(1,\cdot)\|_{L^2(0,1)}\|v(t_j)\|_{L^2(0,1)}.$$

Using this fact in (25), we get, in addition

$$\begin{aligned}
&\|\tilde{v}(t)\|^2_{L^2(0,1)} + \|\tilde{w}(t)\|^2_{L^2(0,1)} \\
&\leq e^{c(t_{j+1}-t_j)}\Big(\|\tilde{v}(t_j)\|^2_{L^2(0,1)} + \|\tilde{w}(t_j)\|^2_{L^2(0,1)} \\
&\quad + \frac{1}{c}\|k(1,\cdot)\|^2_{L^2(0,1)}\|v(t_j)\|^2_{L^2(0,1)}\Big),
\end{aligned}$$

which further gives

$$\begin{aligned}
&\|\tilde{v}(t)\|_{L^2(0,1)} + \|\tilde{w}(t)\|_{L^2(0,1)} \\
&\leq \sqrt{2}e^{\frac{c}{2}(t_{j+1}-t_j)}\Big(\|\tilde{v}(t_j)\|_{L^2(0,1)} + \|\tilde{w}(t_j)\|_{L^2(0,1)} \\
&\quad + \frac{1}{\sqrt{c}}\|k(1,\cdot)\|_{L^2}\|v(t_j)\|_{L^2(0,1)}\Big).
\end{aligned} \tag{26}$$

Thanks to the change of variables (23) and the triangle inequalities, we obtain the following inequalities:

$$\begin{aligned}
\|v(t)\|_{L^2(0,1)} &\leq \|\tilde{v}(t)\|_{L^2(0,1)} + |q_d|, \\
\|\tilde{v}(t_j)\|_{L^2(0,1)} &\leq \|v(t_j)\|_{L^2(0,1)} + |q_d|,
\end{aligned}$$

together with $|q_d| \leq \|k(1,\cdot)\|_{L^2(0,1)}\|v(t_j)\|_{L^2(0,1)}$. Thanks to (26) and the above estimates, we obtain, for all $t \in [t_j, t_{j+1}]$,

$$\begin{aligned}
&\|v(t)\|_{L^2(0,1)} + \|w(t)\|_{L^2(0,1)} \\
&\leq \|\tilde{v}(t)\|_{L^2(0,1)} + \|k(1,\cdot)\|_{L^2(0,1)}\|v(t_j)\|_{L^2(0,1)} + \|\tilde{w}(t)\|_{L^2(0,1)} \\
&\leq \sqrt{2}e^{\frac{c}{2}(t_{j+1}-t_j)}\Big(\|\tilde{v}(t_j)\|_{L^2(0,1)} + \|\tilde{w}(t_j)\|_{L^2(0,1)} \\
&\quad + \frac{1}{\sqrt{c}}\|k\|_{L^2(0,1)}\|v(t_j)\|_{L^2(0,1)}\Big) + \|k(1,\cdot)\|_{L^2(0,1)}\|v(t_j)\|_{L^2(0,1)} \\
&\leq \sqrt{2}e^{\frac{c}{2}(t_{j+1}-t_j)}\Big(\|v(t_j)\|_{L^2(0,1)} + \|k(1,\cdot)\|_{L^2(0,1)}\|v(t_j)\|_{L^2(0,1)} \\
&\quad + \|w(t_j)\|_{L^2(0,1)} + \frac{1}{\sqrt{c}}\|k(1,\cdot)\|_{L^2(0,1)}\|v(t_j)\|_{L^2(0,1)}\Big) \\
&\quad + \|k(1,\cdot)\|_{L^2(0,1)}\|v(t_j)\|_{L^2(0,1)}.
\end{aligned}$$

Therefore, finally, we deduce the following

$$\begin{aligned}
&\sup_{t_j \leq s \leq t_{j+1}}\Big(\|v(s)\|_{L^2(0,1)} + \|w(s)\|_{L^2(0,1)}\Big) \\
&\qquad \leq M_j\Big(\|v(t_j)\|_{L^2(0,1)} + \|w(t_j)\|_{L^2(0,1)}\Big)
\end{aligned}$$

with $M_j = \sqrt{2}e^{\frac{c}{2}(t_{j+1}-t_j)}\left(1 + \|k(1,\cdot)\|_{L^2(0,1)} + \frac{\|k(1,\cdot)\|_{L^2(0,1)}}{\sqrt{c}}\right) + \|k(1,\cdot)\|_{L^2(0,1)}$. This concludes the proof. □

Theorem 4.3. *Under the event-triggered boundary control (19)-(20)-(21), there exists a minimal dwell-time between two triggering times, i.e. there exists a constant $\tau > 0$ (independent of the initial condition (v_0, w_0)) such that $t_{j+1} - t_j \geq \tau$, for all $j \in \mathbb{N}$.*

Proof. Let us consider the following function $g \in C^2([0,1])$

$$g(x) := \sum_{n=1}^{N} k_n\phi_n(x) \tag{27}$$

where $N \in \mathbb{N}$ to be fixed later, $k_n := \int_0^1 k(1,y)\phi_n(y)\mathrm{d}y$, with k satisfying (6) and $\phi_n(x) = \sqrt{2}\sin(n\pi x), n = 1, 2...$ Let us recall (v, w) is the solution of the event-triggered control system (10). Next, we define

$$\tilde{d}(t) = \int_0^1 g(y)\Big(v(t_j, y) - v(t, y)\Big)\,\mathrm{d}y \tag{28}$$

for $t \in [t_j, t_{j+1})$, for $j \in \mathbb{N}$ and g is given by (27). Since $g \in H_0^1(0,1)$ and $v(t_j,\cdot) - v(t,\cdot) \in L^2(0,1) \subset H^{-1}(0,1)$, we can rewrite (28) as

$$\tilde{d}(t) = \Big\langle v(t_j,\cdot) - v(t,\cdot), g\Big\rangle_{-1,1} \tag{29}$$

where $\langle\cdot,\cdot\rangle_{-1,1}$ stands for the usual duality pairing between $H^{-1}(0,1)$ and $H_0^1(0,1)$. Taking the time derivative of $\tilde{d}(t)$ along the solutions of (10) yields, for all $t \in [t_j, t_{j+1})$

$$\begin{aligned}
\dot{\tilde{d}}(t) &= -\langle\partial_t v(t,\cdot), g\rangle_{-1,1} \\
&= -\Big\langle\partial_{yy}v(t,\cdot), g\Big\rangle_{-1,1} + a\int_0^1 v(t,y)g(y)\mathrm{d}y \\
&\quad + \rho\int_0^1 w(t,y)g(y)\mathrm{d}y
\end{aligned}$$

Using the definition of the duality pairing between $H_0^1(0,1)$ and $H^{-1}(0,1)$, we can write the above expression as

$$\begin{aligned}
\dot{\tilde{d}}(t) &= \int_0^1 \partial_y v(t,y)g'(y)\mathrm{d}y + a\int_0^1 v(t,y)g(y)\mathrm{d}y \\
&\quad + \rho\int_0^1 w(t,y)g(y)\mathrm{d}y,
\end{aligned}$$

whence, integrating by parts, we readily have

$$\begin{aligned}
\dot{\tilde{d}}(t) &= v(t,1)g'(1) - v(t,0)g'(0) - \int_0^1 v(t,y)g''(y)\mathrm{d}y \\
&\quad + a\int_0^1 v(t,y)g(y)\mathrm{d}y + \rho\int_0^1 w(t,y)g(y)\mathrm{d}y.
\end{aligned}$$

Noting that $v(t,0) = 0$, $v(t,1) = \int_0^1 k(1,y)v(t_j,y)dy$, and by the expression of g, we get

$$\begin{aligned}\dot{\tilde{d}}(t) = &\int_0^1 k(1,y)v(t_j,y)\mathrm{d}y \sum_{n=1}^{N} k_n\phi_n'(1)\\ &+ \sum_{n=1}^{N} k_n(n^2\pi^2+a)\int_0^1 \phi_n(y)v(t,y)\mathrm{d}y\\ &+ \rho\sum_{n=1}^{N} k_n\int_0^1 \phi_n(y)w(t,y)\mathrm{d}y.\end{aligned}$$

Using the Cauchy-Schwarz inequality and $\|\phi_n\|_{L^2(0,1)} = 1$ for $n = 1, 2, ...$, the following estimate holds for $t \in (t_j, t_{j+1})$, $j \in \mathbb{N}$

$$\begin{aligned}|\dot{\tilde{d}}(t)| \le &\|k(1,\cdot)\|_{L^2(0,1)}\|v(t_j)\|_{L^2(0,1)}F_N\\ &+ \Big(\|v(t)\|_{L^2(0,1)} + \|w(t)\|_{L^2(0,1)}\Big)G_N,\end{aligned} \tag{30}$$

where $F_N := \sum_{n=1}^{N}\left|k_n\phi_n'(1)\right|$ and $G_N := \sum_{n=1}^{N}|k_n(n^2\pi^2+a+\rho)|$. Therefore, from (30) along with the fact $\tilde{d}(t_j) = 0$, we obtain the following estimate:

$$|\tilde{d}(t)| \le (t-t_j)\|k(1,\cdot)\|_{L^2(0,1)}V(t_j)F_N + (t-t_j)\sup_{t_j\le s\le t}(V(s))G_N. \tag{31}$$

Note that using (9) and (28), the deviation $d(t)$ can be expressed as follows:

$$d(t) = \tilde{d}(t) + \int_0^1 (k(1,y)-g(y))(v(t_j,y)-v(t,y))\mathrm{d}y. \tag{32}$$

Hence, combining (31) and (32), we obtain an estimate of d as follows:

$$\begin{aligned}|d(t)| \le &(t-t_j)\|k(1,\cdot)\|_{L^2(0,1)}V(t_j)F_N\\ &+ (t-t_j)\sup_{t_j\le s\le t}(V(s))G_N\\ &+ \|k(1,\cdot)-g\|_{L^2(0,1)}\|v(t_j)\|_{L^2(0,1)}\\ &+ \|k(1,\cdot)-g\|_{L^2(0,1)}\|v(t)\|_{L^2(0,1)}.\end{aligned} \tag{33}$$

Let us first assume that $V(t_j) \neq 0$. Using (33) and assuming that an event is triggered at $t = t_{j+1}$, we have

$$\begin{aligned}|d(t_{j+1})| \le &(t_{j+1}-t_j)\|k(1,\cdot)\|_{L^2(0,1)}V(t_j)F_N\\ &+ (t_{j+1}-t_j)\sup_{t_j\le s\le t_{j+1}}(V(s))G_N\\ &+ \|k(1,\cdot)-g\|_{L^2(0,1)}V(t_j)\\ &+ \|k(1,\cdot)-g\|_{L^2(0,1)}V(t_{j+1})\end{aligned} \tag{34}$$

and, by Definition 4.1, we have that, at $t = t_{j+1}$

$$|d(t_{j+1})| \ge \beta\|k(1,\cdot)\|_{L^2(0,1)}V(t_j) + \beta\|k(1,\cdot)\|_{L^2(0,1)}V(t_{j+1}). \tag{35}$$

Combining (34) and (35), we get

$$\begin{aligned}&\beta\|k(1,\cdot)\|_{L^2(0,1)}V(t_j) + \beta\|k(1,\cdot)\|_{L^2(0,1)}V(t_{j+1})\\ &\le (t_{j+1}-t_j)\|k(1,\cdot)\|_{L^2(0,1)}F_NV(t_j)\\ &\quad + (t_{j+1}-t_j)G_N\sup_{t_j\le s\le t_{j+1}}(V(s))\\ &\quad + \|k(1,\cdot)-g\|_{L^2(0,1)}V(t_j) + \|k(1)-g\|_{L^2(0,1)}V(t_{j+1}),\end{aligned}$$

and hence,

$$\begin{aligned}&\Big(\beta\|k(1,\cdot)\|_{L^2(0,1)} - \|k(1,\cdot)-g\|_{L^2(0,1)}\Big)V(t_{j+1})\\ &\quad + \Big(\beta\|k(1,\cdot)\|_{L^2(0,1)} - \|k(1,\cdot)-g\|_{L^2(0,1)}\Big)V(t_j)\\ &\le (t_{j+1}-t_j)\|k(1,\cdot)\|_{L^2(0,1)}F_NV(t_j)\\ &\quad + (t_{j+1}-t_j)G_N\sup_{t_j\le s\le t_{j+1}}(V(s)).\end{aligned}$$

By the definition of g, $\|k(1,\cdot)-g\|_{L^2(0,1)}$ tends to zero as N tends to infinity. Thus, we can fix a natural number $N \ge 1$ sufficiently large so that $\|k(1,\cdot)-g\|_{L^2(0,1)} < \beta\|k(1,\cdot)\|_{L^2(0,1)}$.

In addition, using the fact that $V(t_{j+1}) \ge 0$ and by (22) in Lemma 4.2, we obtain the following estimate:

$$\begin{aligned}&\Big(\beta\|k(1,\cdot)\|_{L^2(0,1)} - \|k(1,\cdot)-g\|_{L^2(0,1)}\Big)V(t_j)\\ &\quad \le (t_{j+1}-t_j)\|k(1,\cdot)\|_{L^2(0,1)}F_NV(t_j)\\ &\quad\quad + (t_{j+1}-t_j)G_NM_jV(t_j),\end{aligned} \tag{36}$$

where

$$\begin{aligned}M_j = &\sqrt{2}e^{c/2(t_{j+1}-t_j)}\left(1 + \|k(1,\cdot)\|_{L^2(0,1)} + \frac{\|k(1,\cdot)\|_{L^2(0,1)}}{\sqrt{c}}\right)\\ &+ \|k(1,\cdot)\|_{L^2(0,1)}.\end{aligned}$$

Let us define the following quantities

- $a_0 := \beta\|k(1,\cdot)\|_{L^2(0,1)} - \|k(1,\cdot)-g\|_{L^2(0,1)}$,
- $a_1 := \|k(1,\cdot)\|_{L^2(0,1)}F_N + G_N\|k(1,\cdot)\|_{L^2(0,1)}$,
- $a_2 := \sqrt{2}G_N\left(1 + \|k(1,\cdot)\|_{L^2(0,1)} + \frac{\|k(1,\cdot)\|_{L^2(0,1)}}{\sqrt{c}}\right)$,

and after rearranging and rewriting (36), we obtain an inequality of the form

$$0 < a_0 \le a_1(t_{j+1}-t_j) + a_2(t_{j+1}-t_j)e^{\frac{c}{2}(t_{j+1}-t_j)}, \tag{37}$$

from which we aim at finding a lower bound for $(t_{j+1}-t_j)$. Let us denote it as $\alpha(s) := a_1s + a_2se^{\frac{c}{2}s}$ with $s = (t_{j+1}-t_j)$. Since a_0 is strictly positive, then there exists $\tau > 0$ such that $s = (t_{j+1}-t_j) \ge \tau > 0$. Indeed, let us write $\tau = \inf\mathcal{A}$, where $\mathcal{A} = \{s \in (0,\infty) \mid \alpha(s) \ge a_0 > 0\}$. Clearly $\tau \ge 0$. If $\tau = 0$, there exists a sequence $\{s_n\} \in \mathcal{A}$ of nonnegative real numbers such that $s_n \to 0$. As α is continuous function $\alpha(s_n) \to 0$, which is a contradiction to the fact $\alpha(s_n) \ge a_0 > 0$, as $s_n \in \mathcal{A}$.

If $V(t_j) = 0$, then Lemma 4.2 guarantees that $V(t)$ remains zero. In this case, by Definition 4.1, we do not need to employ triggering anymore, and thus, the Zeno phenomenon is immediately excluded. This concludes the proof. □

Thus, we already proved that there is a minimal dwell time (which is uniform and does not depend on either the initial condition or on the state of the system), and no Zeno solution can appear. Henceforth, we have the following result on the existence of solutions of the system (10) with (19)-(20)-(21) for all $t > 0$. The result is the following.

Corollary 4.4. *Let* $(v_0, w_0) \in L^2(0,1) \times L^2(0,1)$. *Then there exists a unique mapping* (v, w) *such that* $(v, w) \in C^0\left([0,\infty); L^2(0,1)\times L^2(0,1)\right)$ *with* $v \in L^2((t_j, t_{j+1}); H^1(0,1))$, *for all* $j \in \mathbb{N}$ *and* (v, w) *satisfies* (10) *for* $t \in (t_j, t_{j+1})$, $\forall j \in \mathbb{N}$.

Proof. The proof follows from the combination of Corollary 3.2 and Theorem 4.3. Indeed, since there is a minimal dwell-time by Theorem 4.3, we can construct a (strictly) sequence of times $\{t_j\}$ given by the rules (19)-(20)-(21) and apply directly Corollary 3.2. □

4.3. Stability analysis

This section is devoted to the main result regarding the exponential stabilization of the linearized FHN system (10). We start by showing that the target system (15) is Input-to-state stable with respect to $d(t)$, defined in (9).

Proposition 4.5 (Input-to-state stability)**.** *Let* $\epsilon \in (0, \delta)$ *be given. Then the target system* (15) *satisfies the following estimate:*

$$\begin{aligned}&\|u(t)\|_{L^2(0,1)} + \|z(t)\|_{L^2(0,1)}\\ &\le Ce^{-\delta t}\left(\|u(0)\|_{L^2(0,1)} + \|z(0)\|_{L^2(0,1)}\right)\\ &\quad + \vartheta \sup_{0\le s\le t}\left(e^{-(\delta-\epsilon)(t-s)}|d(s)|\right),\end{aligned}$$

where $C > 0$ *is uniform with respect to* ϵ *and*

$$\vartheta = \left(2 + \left[\frac{1}{\epsilon} + \frac{2}{\pi^2 + \lambda - \delta + \epsilon}\right]\right). \tag{38}$$

Proof. The continuity of the transformation (11) and the above well-posedness result Corollary 4.4 for the main control system (10) imply that the system (15) has a unique solution (u, z) such that $(u, z) \in C^0\left([0,\infty); L^2(0,1)\times L^2(0,1)\right)$ with $u(t) \in H^1(0,1)$, for a.e. $t \in \left(t_j, t_{j+1}\right)$.
Let us denote $\mathbb{N}^* = \mathbb{N} \setminus \{0\}$ and write

$$\begin{aligned}u_n(t) &= \sqrt{2}\int_0^1 u(t,x)\sin(n\pi x)\mathrm{d}x,\\ z_n(t) &= \sqrt{2}\int_0^1 z(t,x)\sin(n\pi x)\mathrm{d}x.\end{aligned}$$

As $\left\{\sqrt{2}\sin(n\pi x)\right\}_{n\in\mathbb{N}^*}$ forms an orthonormal basis of $L^2(0,1)$, using Parseval's identity we have that

$$\|u(t)\|^2_{L^2(0,1)} = \sum_{n=1}^{\infty}|u_n(t)|^2,\ \|z(t)\|^2_{L^2(0,1)} = \sum_{n=1}^{\infty}|z_n(t)|^2. \tag{39}$$

Then (u_n, z_n) satisfy the following equation:

$$\begin{cases}\dot{u}_n(t) + (n^2\pi^2 + \lambda)u_n(t) + \rho z_n(t) = (-1)^n n\pi d(t),\\ \dot{z}_n(t) + \delta z_n(t) = \gamma u_n(t).\end{cases}$$

Let us write the above system in the following abstract form

$$\begin{cases}\dot{\mathbf{U}}_n(t) = A_n\mathbf{U}_n(t) + F_n(t), \mathbf{U}_n(t) = (u_n(t), z_n(t))^T,\\ \mathbf{U}_n(0) = (u_{n,0}, z_{0,n})^T.\end{cases} \tag{40}$$

where

$$A_n = \begin{bmatrix}-(n^2\pi^2 + \lambda) & -\rho\\ \gamma & -\delta\end{bmatrix},\quad F_n(t) = ((-1)^n n\pi d(t), 0)^T.$$

We decompose A_n as

$$A_n = \begin{bmatrix}-\delta & 0\\ 0 & -\delta\end{bmatrix} + \begin{bmatrix}-(n^2\pi^2 + \lambda - \delta) & -\rho\\ \gamma & 0\end{bmatrix} = A_1 + B_n.$$

Since the matrix A_1 and B_n commute, we have $e^{A_n t} = e^{A_1 t}e^{B_n t}$. For each $n \in \mathbb{N}^*$, the eigenvalues of the matrix B_n are given by

$$\begin{aligned}\lambda_n &= \frac{1}{2}\left[-(\lambda + n^2\pi^2 - \delta) + \left(\sqrt{(\lambda + n^2\pi^2 - \delta)^2 - 4\rho\gamma}\right)\right],\\ \mu_n &= \frac{1}{2}\left[-(\lambda + n^2\pi^2 - \delta) - \left(\sqrt{(\lambda + n^2\pi^2 - \delta)^2 - 4\rho\gamma}\right)\right].\end{aligned}$$

We choose the damping parameter λ large enough. In particular, we set λ in such a way that

$$\lambda - \delta > 2\sqrt{\rho\gamma}. \tag{41}$$

It can be easily checked that the eigenvalues of the matrix B_n are negative for all $n \in \mathbb{N}^*$. Furthermore, for large values of n, we have the following behavior of the eigenvalues of B_n

$$\begin{aligned}\lambda_n &\approx -\frac{\rho\gamma}{n^2\pi^2} + O\left(\frac{1}{n^4}\right),\\ \mu_n &\approx -(n^2\pi^2 + \lambda - \delta) + O\left(\frac{1}{n^2}\right).\end{aligned}$$

Also we have

$$\begin{aligned}(\lambda_n - \mu_n) &= \sqrt{(\lambda + n^2\pi^2 - \delta)^2 - 4\rho\gamma} > 0\\ &\quad \text{(by the choice of } \lambda\text{, see (41))}\end{aligned}$$

and the following asymptotic expression

$$(\lambda_n - \mu_n) \approx n^2\pi^2 + \lambda - \delta - \frac{2\rho\gamma}{n^2\pi^2} + O\left(\frac{1}{n^4}\right).$$

A direct computation shows that,

$$e^{B_n t} = \frac{1}{\lambda_n - \mu_n}\begin{bmatrix}\lambda_n e^{\lambda_n t} - \mu_n e^{\mu_n t} & \frac{\lambda_n\mu_n}{\gamma}\left(e^{\mu_n t} - e^{\lambda_n t}\right)\\ \gamma(e^{\lambda_n t} - e^{\mu_n t}) & \lambda_n e^{\mu_n t} - \mu_n e^{\lambda_n t}\end{bmatrix}$$

for all $n \in \mathbb{N}^*$. Therefore,

$$e^{A_n t} = \frac{1}{\lambda_n - \mu_n}e^{-\delta t}\begin{bmatrix}\lambda_n e^{\lambda_n t} - \mu_n e^{\mu_n t} & \frac{\lambda_n\mu_n}{\gamma}\left(e^{\mu_n t} - e^{\lambda_n t}\right)\\ \gamma(e^{\lambda_n t} - e^{\mu_n t}) & \lambda_n e^{\mu_n t} - \mu_n e^{\lambda_n t}\end{bmatrix}.$$

The corresponding solution $\mathbf{U}_n(t)$ of (40) is given by

$$\mathbf{U}_n(t) = e^{A_n t}\mathbf{U}_0 + \int_0^t e^{A_n(t-s)}F_n(s)\mathrm{d}s.$$

Thus we have the following expressions for the solution of (40):

$$
\begin{aligned}
&u_n(t)\\
&=\frac{e^{-\delta t}}{\lambda_n-\mu_n}\Big[u_{0,n}(\lambda_n e^{\lambda_n t}-\mu_n e^{\mu_n t})+\frac{\lambda_n\mu_n}{\gamma}z_{0,n}(e^{\mu_n t}-e^{\lambda_n t})\Big]\\
&\quad+\frac{(-1)^n n\pi}{\mu_n-\lambda_n}\int_0^t e^{-\delta(t-s)}\left(\lambda_n e^{\lambda_n(t-s)}-\mu_n e^{\mu_n(t-s)}\right)d(s)\mathrm{d}s,\\
&z_n(t)\\
&=\frac{e^{-\delta t}}{\lambda_n-\mu_n}\Big[u_{0,n}\gamma(e^{\lambda_n t}-e^{\mu_n t})+z_{0,n}(\lambda_n e^{\mu_n t}-\mu_n e^{\lambda_n t})\Big]\\
&\quad+\frac{(-1)^n n\pi\gamma}{\lambda_n-\mu_n}\int_0^t e^{-\delta(t-s)}\left(e^{\lambda_n(t-s)}-e^{\mu_n(t-s)}\right)d(s)\mathrm{d}s.
\end{aligned}
$$

In order to find the stability estimate for the system (15), it is enough to establish the same for (u_n, z_n), the solution of (40).

Estimate of $u_n(t)$. By direct computations, we have

$$
\begin{aligned}
&|u_n(t)|^2\\
&\le\frac{e^{-2\delta t}}{|\mu_n-\lambda_n|^2}\Big[|u_{0,n}|^2(\lambda_n e^{\lambda_n t}-\mu_n e^{\mu_n t})^2\\
&\quad+|z_{0,n}|^2\rho^2\gamma(e^{\lambda_n t}-e^{\mu_n t})^2\Big]\\
&\quad+\frac{n^2\pi^2}{|\mu_n-\lambda_n|^2}\left(\int_0^t e^{-\delta(t-s)}\left(\lambda_n e^{\lambda_n(t-s)}-\mu_n e^{\mu_n(t-s)}\right)d(s)\mathrm{d}s\right)^2\\
&\le Ce^{-2\delta t}\Big[|z_{0,n}|^2\frac{(|\lambda_n|^2+|\mu_n|^2)}{|\mu_n-\lambda_n|^2}+|u_{0,n}|^2\frac{2}{|\mu_n-\lambda_n|^2}\Big]\\
&\quad+\frac{n^2\pi^2}{|\mu_n-\lambda_n|^2}\mathcal{I}^2.
\end{aligned}
\tag{42}
$$

Let us estimate the term $\mathcal{I}=\int_0^t e^{-\delta(t-s)}\left(\lambda_n e^{\lambda_n(t-s)}-\mu_n e^{\mu_n(t-s)}\right)d(s)\mathrm{d}s$.

$$
\begin{aligned}
|\mathcal{I}|&\le\sup_{0\le s\le t}\left(e^{-\delta(t-s)}|d(s)|\right)\int_0^t\left|\left(\lambda_n e^{\lambda_n(t-s)}-\mu_n e^{\mu_n(t-s)}\right)\right|\mathrm{d}s\\
&\le\sup_{0\le s\le t}\left(e^{-\delta(t-s)}|d(s)|\right)\left(\frac{|\lambda_n|}{\lambda_n}(e^{\lambda_n t}-1)+\frac{|\mu_n|}{\mu_n}(e^{\mu_n t}-1)\right)\\
&\le 2\sup_{0\le s\le t}\left(e^{-\delta(t-s)}|d(s)|\right),
\end{aligned}
\tag{43}
$$

here we have used the fact $\left|\left(\frac{|\lambda_n|}{\lambda_n}(e^{\lambda_n t}-1)+\frac{|\mu_n|}{\mu_n}(e^{\mu_n t}-1)\right)\right|<2$ as $\lambda_n,\mu_n<0$.

Therefore combining (42) and (43), we get

$$
\begin{aligned}
|u_n(t)|^2&\le C_1e^{-2\delta t}\left[|u_{0,n}|^2+|z_{0,n}|^2\right]\\
&\quad+\frac{4n^2\pi^2}{|\mu_n-\lambda_n|^2}\left(\sup_{0\le s\le t}\left(e^{-\delta(t-s)}|d(s)|\right)\right)^2,
\end{aligned}
\tag{44}
$$

for a constant $C_1>0$ independent of n, where we have used the expressions of μ_n,λ_n to bound the quantities $\frac{(|\lambda_n|^2+|\mu_n|^2)}{|\mu_n-\lambda_n|^2}$ and $\frac{2}{|\mu_n-\lambda_n|^2}$ appearing in (42).

Estimate of $z_n(t)$. Similarly, we have

$$
\begin{aligned}
&|z_n(t)|^2\\
&\le\frac{e^{-2\delta t}}{|\mu_n-\lambda_n|^2}\Big[|u_{0,n}|^2\gamma^2(e^{\lambda_n t}-e^{\mu_n t})^2\\
&\quad+|z_{0,n}|^2(\lambda_n e^{\mu_n t}-\mu_n e^{\lambda_n t})^2\Big]\\
&\quad+\frac{n^2\pi^2}{|\mu_n-\lambda_n|^2}\left(\int_0^t e^{-\delta(t-s)}\left(e^{\lambda_n(t-s)}-e^{\mu_n(t-s)}\right)d(s)\mathrm{d}s\right)^2\\
&\le Ce^{-2\delta t}\Big[|z_{0,n}|^2\frac{(|\lambda_n|^2+|\mu_n|^2)}{|\mu_n-\lambda_n|^2}+|u_{0,n}|^2\frac{2}{|\mu_n-\lambda_n|^2}\Big]\\
&\quad+\frac{n^2\pi^2}{|\mu_n-\lambda_n|^2}\mathcal{J}^2.
\end{aligned}
\tag{45}
$$

Let $\epsilon\in(0,\delta)$ be given. We estimate the term $\mathcal{J}=\int_0^t e^{-\delta(t-s)}\left(e^{\lambda_n(t-s)}-e^{\mu_n(t-s)}\right)d(s)\mathrm{d}s$ as follows

$$
\begin{aligned}
|\mathcal{J}|&\le\sup_{0\le s\le t}\left(e^{-(\delta-\epsilon)(t-s)}|d(s)|\right)\Big(e^{(\lambda_n-\epsilon)t}\int_0^t e^{-(\lambda_n-\epsilon)s}\\
&\qquad+e^{(\mu_n-\epsilon)t}\int_0^t e^{-(\mu_n-\epsilon)s}\Big)\\
&\le\sup_{0\le s\le t}\left(e^{-(\delta-\epsilon)(t-s)}|d(s)|\right)\left(\frac{e^{(\lambda_n-\epsilon)t}-1}{(\lambda_n-\epsilon)}+\frac{e^{(\mu_n-\epsilon)t}-1}{(\mu_n-\epsilon)}\right)\\
&\le M_2\sup_{0\le s\le t}\left(e^{-(\delta-\epsilon)(t-s)}|d(s)|\right),
\end{aligned}
\tag{46}
$$

where $M_2=\sup_{t>0}\left(\frac{e^{(\lambda_n-\epsilon)t}-1}{(\lambda_n-\epsilon)}+\frac{e^{(\mu_n-\epsilon)t}-1}{(\mu_n-\epsilon)}\right)$. Therefore combining (45) and (46), we have

$$
\begin{aligned}
|z_n(t)|^2&\le C_1e^{-2\delta t}[|u_{0,n}|^2+|z_{0,n}|^2]\\
&\quad+(M_2)^2\frac{n^2\pi^2}{|\mu_n-\lambda_n|^2}\left(\sup_{0\le s\le t}\left(e^{-(\delta-\epsilon)(t-s)}|d(s)|\right)\right)^2.
\end{aligned}
\tag{47}
$$

Using the expressions of the eigenvalues and noting the fact that $\lambda_n,\mu_n<0$, we have $M_2\le\left[\frac{1}{\epsilon}+\frac{2}{\pi^2+\lambda-\delta+\epsilon}\right]$. Adding (44) and (47), we deduce

$$
\begin{aligned}
\sum_{n=1}^{\infty}|u_n(t)|^2+\sum_{n=1}^{\infty}|z_n(t)|^2&\le 2C_1e^{-2\delta t}\Big[\sum_{n=1}^{\infty}|u_{0,n}|^2+\sum_{n=1}^{\infty}|z_{0,n}|^2\Big]\\
&\quad+((M_2)^2+4)\left(\sup_{0\le s\le t}\left(e^{-(\delta-\epsilon)(t-s)}|d(s)|\right)\right)^2\sum_{n=1}^{\infty}\frac{n^2\pi^2}{|\mu_n-\lambda_n|^2}.
\end{aligned}
\tag{48}
$$

Let us estimate the following term

$$
\begin{aligned}
&|\lambda_n-\mu_n|^2\\
&=n^4\pi^4\left(1+\frac{\lambda-\delta}{n^2\pi^2}+\frac{2\sqrt{\rho\gamma}}{n^2\pi^2}\right)\left(1+\frac{\lambda-\delta}{n^2\pi^2}-\frac{2\sqrt{\rho\gamma}}{n^2\pi^2}\right)\ge n^4\pi^4.
\end{aligned}
$$

Using (39), (48), and the above estimate yields

$$
\begin{aligned}
&\|u(t)\|^2_{L^2(0,1)}+\|z(t)\|^2_{L^2(0,1)}\\
&\le C_2e^{-2\delta t}\left(\|u_0\|^2_{L^2(0,1)}+\|z_0\|^2_{L^2(0,1)}\right)\\
&\quad+\left((M_2)^2+4\right)\left(\sup_{0\le s\le t}\left(e^{-(\delta-\epsilon)(t-s)}|d(s)|\right)\right)^2.
\end{aligned}
$$

The required result follows from a direct computation. □

Remark 4.6. *The constant ϑ in the input-to-state stability estimate Proposition 4.5 is not sharp. The reason for getting such a bound is that we need to use an upper bound of the term M_2 in the estimate of z_n, see (47). In other cases, such as for scalar parabolic equations, an explicit bound for ϑ can be derived, depending on the system parameters and the decay rate. For further details, see [16, Lemma 3].*

Remark 4.7. *We have chosen the damping parameter λ (see (41)) present in the target equation (15) in such a way that for each $n \in \mathbb{N}^*$, the eigenvalue of the matrix B_n are real and negative as well. It simplifies the computation in the estimate of u_n and z_n of the above proof. Otherwise, as we seek to get the stability of (15) with decay up to $\omega < \delta$, the assumption $\lambda > \delta$ is enough.*

Now we are in a position to prove our main exponential stabilization result.

Theorem 4.8. *Let $\epsilon \in (0, \delta)$ be given, ϑ be as in Proposition 4.5 and β be chosen in such a way that*

$$\Phi_e := 2\beta\vartheta\|k(1,\cdot)\|_{L^2(0,1)}\|\Pi^{-1}\|_{L^2\mapsto L^2} < 1. \tag{49}$$

Then, the closed-loop system (10) with event-triggered boundary control (19)-(21) has a unique solution and is globally exponentially stable, i.e. there exists $M > 0$ depending on ϵ and the system parameters such that for every $(v_0, w_0) \in L^2(0,1) \times L^2(0,1)$ the unique solution $(v, w) \in C^0([0,\infty); L^2(0,1) \times L^2(0,1))$ of (10) satisfies

$$\begin{aligned}&\|v(t)\|_{L^2(0,1)} + \|w(t)\|_{L^2(0,1)}\\ &\le Me^{-(\delta-\epsilon)t}\left(\|v(0)\|_{L^2(0,1)} + \|w(0)\|_{L^2(0,1)}\right), \text{ for all } t \ge 0.\end{aligned} \tag{50}$$

Remark 4.9. *Note that in Theorem 4.8 we prove the exponential decay $e^{-\omega t}$ with $\omega = \delta - \epsilon$ for all $\epsilon \in (0, \delta)$ for the closed-loop system (10) with even-triggered control. In this regard, we can always choose $\epsilon > 0$ small enough such that $a < \delta - \epsilon$. This improves the decay rate of the open-loop system (i.e., (2) with $q = 0$).*

Remark 4.10. *In practice, the good strategy to choose the free parameters involved in the event-triggering control design is as follows:*

1. *We choose $\epsilon > 0$ small enough according to the discussion in Remark 4.9.*
2. *We fix λ sufficiently large as in (41), which only depends on the system parameters δ, ρ and γ.*
3. *We compute the constant ϑ in (38) of Proposition 4.5 (depending on ϵ and λ).*
4. *Lastly, we compute β according to (49) in Theorem 4.8.*

Remark 4.11. *Note that as $\epsilon \searrow 0$, the parameter ϑ in Proposition 4.5 grows to infinity. This implies that we must choose the parameter β in (49) to be very small, which, according to Definition 4.1, leads to more triggering events occurring and the dwell-time decreasing to 0.*

Proof of Theorem 4.8. For given $\epsilon \in (0, \delta)$, we set ϑ as in Proposition 4.5 and, to abridge the notation, we denote $\nu = \delta - \epsilon$. It follows from (20) that the following inequality holds for all $t \in [t_j, t_{j+1})$

$$|d(t)| \le \beta\|k(1,\cdot)\|_{L^2(0,1)}V(t_j) + \beta\|k(1,\cdot)\|_{L^2(0,1)}V(t). \tag{51}$$

For every $t \ge 0$, we define $f(t) = \max\{t_j : j \in \mathbb{N}, t \ge t_j\}$. Then, inequality (51) implies the following

$$|d(t)| \le \beta\|k(1,\cdot)\|_{L^2(0,1)}V(f(t)) + \beta\|k(1,\cdot)\|_{L^2(0,1)}V(t). \tag{52}$$

Therefore, from (52), we deduce the following inequality for all $t \ge 0$

$$\left(|d(t)|e^{\nu t}\right) \le 2\beta\|k(1,\cdot)\|_{L^2(0,1)} \sup_{0\le s\le t}\left(V(s)e^{\nu s}\right). \tag{53}$$

Let us choose any $\hat{t} \ge 0$. Then for all $t \in [0, \hat{t}]$ we have from (53)

$$\left(|d(t)|e^{\nu t}\right) \le 2\beta\|k(1,\cdot)\|_{L^2(0,1)} \sup_{0\le s\le \hat{t}}\left(V(s)e^{\nu s}\right). \tag{54}$$

As the above estimate holds for all $t \in [0, \hat{t}]$, we have

$$\sup_{0\le s\le \hat{t}}\left(|d(s)|e^{\nu s}\right) \le 2\beta\|k(1,\cdot)\|_{L^2(0,1)} \sup_{0\le s\le \hat{t}}\left(V(s)e^{\nu s}\right). \tag{55}$$

Since $\hat{t}$ is arbitrary, one can write the following

$$\sup_{0\le s\le t}\left(|d(s)|e^{\nu s}\right) \le 2\beta\|k(1,\cdot)\|_{L^2(0,1)} \sup_{0\le s\le t}\left(V(s)e^{\nu s}\right). \tag{56}$$

On the other hand, by Proposition 4.5 and a direct computation, we obtain

$$\begin{aligned}&\left(\|u(t)\|_{L^2} + \|z(t)\|_{L^2}\right)e^{\nu t}\\ &\quad\le C\left(\|u(0)\|_{L^2} + \|z(0)\|_{L^2}\right) + \vartheta \sup_{0\le s\le t}\left(|d(s)|e^{\nu s}\right).\end{aligned} \tag{57}$$

Again let us pick $\hat{t} \ge 0$. Then for all $t \in [0, \hat{t}]$, we have

$$\begin{aligned}&\left(\|u(t)\|_{L^2} + \|z(t)\|_{L^2}\right)e^{\nu t}\\ &\quad\le C\left(\|u(0)\|_{L^2} + \|z(0)\|_{L^2}\right) + \vartheta \sup_{0\le s\le \hat{t}}\left(|d(s)|e^{\nu s}\right).\end{aligned} \tag{58}$$

As the above estimate holds for all $t \in [0, \hat{t}]$, we have

$$\begin{aligned}&\sup_{0\le s\le \hat{t}}\left(\|u(s)\|_{L^2} + \|z(s)\|_{L^2}\right)e^{\nu s}\\ &\quad\le C\left(\|u(0)\|_{L^2} + \|z(0)\|_{L^2}\right) + \vartheta \sup_{0\le s\le \hat{t}}\left(|d(s)|e^{\nu s}\right).\end{aligned} \tag{59}$$

Since $\hat{t}$ is arbitrary, we can write the following

$$\begin{aligned}&\sup_{0\le s\le t}\left(\left(\|u(s)\|_{L^2} + \|z(s)\|_{L^2}\right)e^{\nu s}\right)\\ &\quad\le C\left(\|u(0)\|_{L^2} + \|z(0)\|_{L^2}\right) + \vartheta \sup_{0\le s\le t}\left(|d(s)|e^{\nu s}\right).\end{aligned} \tag{60}$$

Hence, combining (56) with (60), we obtain

$$\begin{aligned}&\sup_{0\le s\le t}\left(\left(\|u(s)\|_{L^2} + \|z(s)\|_{L^2}\right)e^{\nu s}\right)\\ &\quad\le C\left(\|u(0)\| + \|z(0)\|_{L^2}\right) + 2\beta\vartheta\|k(1,\cdot)\|_{L^2} \sup_{0\le s\le t}\left(V(s)e^{\nu s}\right)\end{aligned}$$

and using the fact $V(s) \leq \Pi^{-1}(\|u(t)\| + \|z(t)\|)$, we deduce

$$\begin{aligned}&\sup_{0\leq s\leq t}\left((\|u(s)\|_{L^2} + \|z(s)\|_{L^2})\, e^{\nu s}\right)\\ &\quad\leq C\left(\|u(0)\|_{L^2} + \|z(0)\|_{L^2}\right)\\ &\qquad + \Phi_e \sup_{0\leq s\leq t}\left((\|u(s)\|_{L^2} + \|z(s)\|_{L^2})\, e^{\nu s}\right),\end{aligned}$$

where $\Phi_e := 2\beta\vartheta\|k(1,\cdot)\|_{L^2}\|\Pi^{-1}\|_{L^2\mapsto L^2}$. Thereby, thanks to (49) and the invertibility of the backstepping transformation, the solution to the closed-loop system (10) with event-triggered control (20)-(21) satisfies

$$\begin{aligned}&\sup_{0\leq s\leq t}\left((\|v(s)\|_{L^2} + \|w(s)\|_{L^2})\, e^{\nu s}\right)\\ &\quad\leq C\,\|\Pi\|_{L^2\mapsto L^2}\left\|\Pi^{-1}\right\|_{L^2\mapsto L^2}(1-\Phi_e)^{-1}\\ &\qquad\times\left(\|v(0)\|_{L^2} + \|w(0)\|_{L^2}\right),\end{aligned}$$

which leads to the following:

$$\begin{aligned}&\left(\|v(t)\|_{L^2} + \|w(t)\|_{L^2}\right)\\ &\quad\leq Me^{-\nu t}\left(\|v(0)\|_{L^2} + \|w(0)\|_{L^2}\right),\ \forall t\geq 0,\end{aligned}$$

with $M := C\,\|\Pi\|_{L^2\mapsto L^2}\left\|\Pi^{-1}\right\|_{L^2\mapsto L^2}(1-\Phi_e)^{-1}$. The proof is finished. □

5. Numerical experiments

In this section, we present some numerical illustrations and comments about the practical implementation of the backstepping technique and the event-triggering control. In what follows we shall use the notation $[\![a,b]\!] = [a,b]\cap\mathbb{N}$ for any real numbers $a < b$.

5.1. Some considerations on the system parameters

In Section 1.3, we have mentioned that the linearized FitzHugh-Nagumo system (2) is exponentially stable with a decay rate $\omega = \min\{a,\delta\}$ without the action of any control. Thus the important case to study the backstepping-based stabilization problem is when $a < \delta$. As, in this case, the free system ((2) with $q = 0$) is stable with exponential decay e^{-at}, and the action of the event-triggering control law makes the decay rate up to $e^{-\omega t}$, $\omega < \delta$.

To see the effect, in a numerical simulation, of the action of the event-triggering control law, that actually helps to stabilize an unstable system to a stable one, we choose to change the sign of the parameters a in the system (2) and make the stable FHN to an unstable coupled parabolic-ODE system. To this end, let us consider the model given by

$$\begin{cases}\partial_t v = \partial_x^2 v - av - \rho w, & \text{in } (0,\infty)\times(0,1),\\ \partial_t w = \gamma v - \delta w, & \text{in } (0,\infty)\times(0,1),\\ v(t,0) = 0, \quad v(t,1) = q(t) & \text{in } (0,\infty),\\ v(0,x) = v_0(x), & \text{in } (0,1),\\ w(0,x) = w_0(x) & \text{in } (0,1),\end{cases} \tag{61}$$

where $\rho,\gamma > 0$ and $\delta > 0 > a$. For some fixed values of ρ,γ,δ, we choose $a < 0$ in such a way that it satisfies the following

$$\begin{aligned}&(a+\pi^2-\delta)^2 - 4\rho\gamma > 0\\ &\text{along with } \sqrt{(a+\pi^2-\delta)^2-4\rho\gamma} > (a+\pi^2+\delta).\end{aligned} \tag{62}$$

As a is negative, we can always choose such a with a large enough absolute value. Furthermore, the spectrum of the associated operator for the system (61) can be expressed as

$$\begin{aligned}\lambda_n &= \frac{1}{2}\Big[-\left(a+n^2\pi^2+\delta\right) + \sqrt{(a+n^2\pi^2-\delta)^2-4\rho\gamma}\Big],\\ \mu_n &= \frac{1}{2}\Big[-\left(a+n^2\pi^2+\delta\right) - \sqrt{(a+n^2\pi^2-\delta)^2-4\rho\gamma}\Big].\end{aligned}$$

These expressions suggest that it is reasonable to find the conditions for a for which the first eigenvalue for λ_n is positive. Thanks to the assumption (62), we have $\lambda_1 > 0$, which essentially ensures the instability of the system (61).

It is worth mentioning that, here, we will not change the sign of the ODE component in the ODE of the system (2). Otherwise, it is impossible to make the system exponentially stable, as indeed, the continuous backstepping-based feedback law also could not change the decay rate of the ODE, see [5].

5.2. Discretization of the coupled model and numerical implementation of the backstepping control

For the numerical tests, system (61) is discretized in time by using a standard implicit Euler scheme and discretized in space by a usual finite-difference scheme. More precisely, let $N, M \in \mathbb{N}^*$, we set $\delta t = T/M$ and $h = 1/(N+1)$ and consider the following uniform discretization for the space and time variables

$$\begin{aligned}&0 = x_0 < x_1 < \ldots < x_N < x_{N+1} = 1,\\ &0 = t_0 < t_1 < \ldots < T_M = T,\end{aligned}$$

where $x_i = ih$, $i \in [\![0, N+1]\!]$, and $t_n = n\delta t$, $n \in [\![0, M]\!]$. The numerical approximation of a function $f = f(x,t)$ at a grid point (t_n, x_i) will be denoted as $f_i^n := f(t_n, x_i)$ and, for fixed n, we write $f^n = \left(\begin{array}{c} f_1^n,\ldots,f_N^n\end{array}\right)^\top$ the evaluation at the interior points.

Defining $Z := (v,w)^\top$ and using the above notation, the fully-discrete version of (61) takes the form

$$\begin{cases}\dfrac{Z^{n+1}-Z^n}{\delta t} + \mathcal{A}_h Z^{n+1} = \mathcal{B}_h q^{n+1}, & n\in[\![0,M-1]\!]\\ Z^0 = Z_h^0,\end{cases} \tag{63}$$

where $(Z^n)_{n\in[\![0,M]\!]} \subset \mathbb{R}^2\otimes\mathbb{R}^N$ and $(q^n)_{n\in[\![1,M]\!]} \subset \mathbb{R}$ are the (discrete) state and control variables, respectively, $Z_h^0 \in \mathbb{R}^2\otimes\mathbb{R}^N$ is the approximation of the initial data (v_0, w_0), the (boundary) control operator $\mathcal{B}_h \in \mathbb{R}^2\otimes R^N$ is given by

$$\mathcal{B}_h = \frac{1}{h^2}\begin{pmatrix}1\\0\end{pmatrix}\otimes\begin{pmatrix}0\\0\\\vdots\\1\end{pmatrix}_N,$$

and $\mathcal{A}_h \in \mathbb{R}^{2\times 2} \otimes \mathbb{R}^{N\times N}$ is

$$\mathcal{A}_h = \begin{pmatrix} 1 & 0 \\ 0 & 0 \end{pmatrix} \otimes \mathcal{A}_{h,D} + \mathsf{C} \otimes I_{N\times N},$$

where $\mathcal{A}_{h,D} \in \mathbb{R}^{N\times N}$ is the usual tridiagonal matrix coming from the discretization of the Laplacian operator $-\partial_{xx}$ with homogeneous Dirichlet boundary conditions, that is, $(\mathcal{A}_h y)_i = -\frac{1}{h^2}(y_{i+1} - 2y_i + y_{i-1})$, $i = [\![1, N]\!]$ and $\mathsf{C} = \begin{pmatrix} a & \rho \\ -\gamma & \delta \end{pmatrix}$ are the coupling coefficients.

Now, let us turn our attention to the control part. Recall that the backstepping control is given by the explicit feedback control law

$$q(t) = \int_0^1 k(1, y)v(t, y)\mathrm{d}y, \tag{64}$$

where $k = k(x, y)$ is the solution to (6). This particular structure simplifies the implementation of the control. In fact, we can approximate (64) directly at a time-grid point t_n (i.e., $q(t_n) = q^n$) with the formula

$$q^n = h\sum_{i=1}^{N} k(1, x_i)v_i^n. \tag{65}$$

Remark 5.1. *There are, of course, different ways to discretize the integral in (64). For instance the trapezoidal rule would slightly modify (65), specifically,*

$$q^n = \frac{h}{1 - \frac{h\varpi}{2}} \sum_{i=1}^{N} k(1, x_i)v_i^n, \quad n \in [\![1, M]\!].$$

where $\varpi = a - \lambda < 0$. We opted for (65) due to its simplicity in numerical implementation.

Note that (65) can be written in compact form and using the complete state variable Z by introducing the vector $K \in \mathbb{R}^2 \otimes \mathbb{R}^N$ defined by

$$K^\top := \begin{pmatrix} k_{1,1} & k_{1,2} & \dots & k_{1,N} & 0 & 0 & \cdots & 0 \end{pmatrix} \tag{66}$$

where $k_{1,i} := k(1, x_i)$. More precisely,

$$q^n = hK^\top Z^n, \quad n \in [\![1, M]\!]. \tag{67}$$

Thus, combining (63) and (67), the feedback control system simplifies to

$$\begin{cases} \dfrac{Z^{n+1} - Z^n}{\delta t} + \left(\mathcal{A}_h - h\mathcal{B}_h K^\top\right) Z^{n+1} = 0, \quad n \in [\![0, M-1]\!], \\ Z^0 = Z_h^0. \end{cases} \tag{68}$$

To illustrate the behavior of the controlled system (61), let us choose the following parameters: we set

$$T = 6, \quad v_0(x) = \sin(\pi x), \quad w_0(x) = \sin(2\pi x), \tag{69}$$

and the coupling matrix

$$\mathsf{C} = \begin{pmatrix} -11 & 1 \\ -1 & 1 \end{pmatrix}, \tag{70}$$

where we choose the entries in the matrix C according to the constraints (62).

With these parameters, it can be verified that the uncontrolled system (setting $q \equiv 0$) is unstable, as shown in Figure 1. Such figures have been obtained with the help of the numerical scheme (68) with parameters $N = 40$, $M = 4000$[3] and setting $\mathcal{B}_h \equiv 0$ for observing the uncontrolled dynamics.

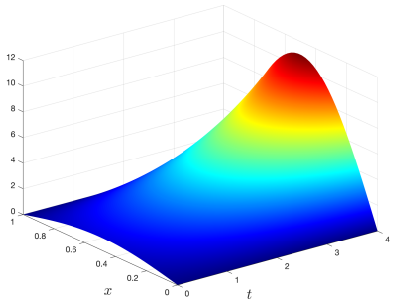

(a) The PDE component $(t, x) \mapsto v(t, x)$.

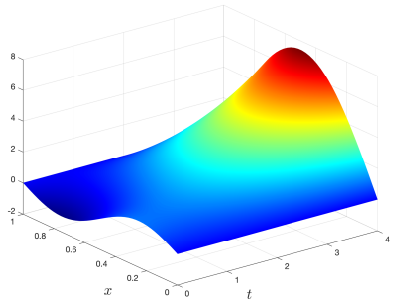

(b) The ODE component $(t, x) \mapsto w(t, x)$.

Figure 1: Evolution in time of the uncontrolled system (61).

Now, we choose $\lambda = 4$, compute K as in (66) with the help of formula (7) and use the numerical scheme (68) to illustrate the behavior of the closed-loop system, see Figure 2. We see that by applying the boundary control shown in Figure 2c the system becomes stable.

Unlike other similar backstepping control problems, as noted in [5], the best achievable exponential rate for our closed-loop system with backstepping control is determined by the decay of the ODE component in (61). In other words, we cannot attain an arbitrary exponential decay rate regardless of the control design. To illustrate this, we have computed feedback controls with different design parameters λ, and compared the dynamics, as shown in Figure 3. Even though the dynamics are distinct at the very beginning of the time interval, after some point, all dynamics converge and become almost identical. The figure effectively illustrates this convergence behavior.

5.3. Numerical illustration of the event-triggering control

With the discrete system given in (63) and the backstepping control law defined by (67), we can easily adapt our compu-

[3] These simulation parameters will be used in the remainder of the simulations shown in this section, unless otherwise specified.

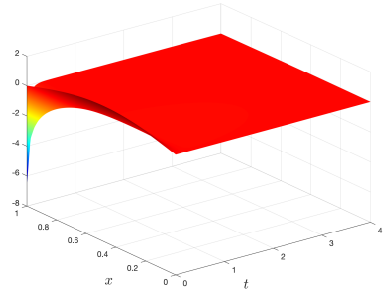

(a) The PDE component $(t, x) \mapsto v(t, x)$.

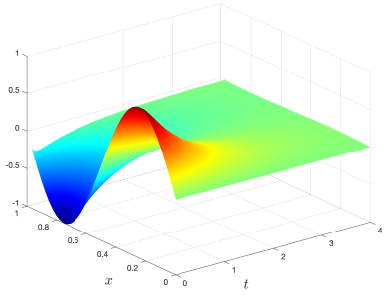

(b) The ODE component $(t, x) \mapsto w(t, x)$.

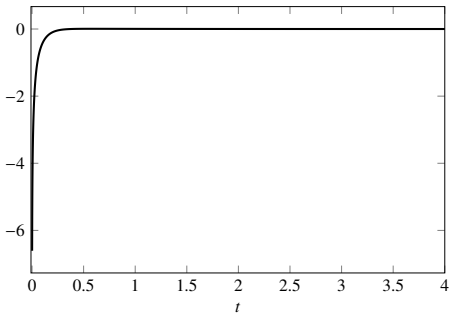

(c) The control $t \mapsto q(t)$.

Figure 2: Evolution in time of the controlled system (61) with backstepping control (64).

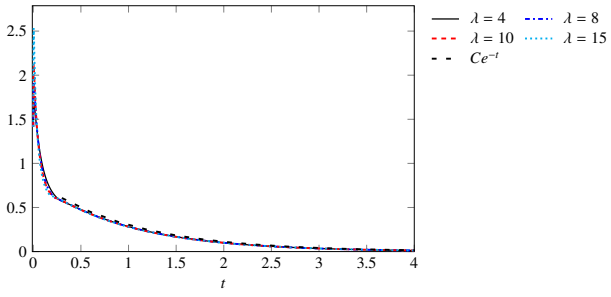

Figure 3: Norm of the closed-loop dynamics $t \mapsto \|v(t)\|_{L^2} + \|w(t)\|_{L^2}$ of (61) with different design parameters λ. For comparison, we have added the exponential function Ce^{-t} for some $C > 0$, which is the best theoretical decay rate for system (61) with coupling parameters (70).

tation tool to address the event-triggering problem. For clarity and future reference, we present a brief pseudocode in Algorithm 1 that outlines the essential steps.

Algorithm 1 Event-triggered control with backstepping

Input: Initial (discrete) states (v_0, w_0); discrete parameters h, δt (resp. N, M); matrices C, $\mathcal{A}_h$, $\mathcal{B}_h$, K; time $T > 0$, parameter β

Initialize:

  Set $v^0 \leftarrow u_0$, $w^0 \leftarrow w_0$ and arrange in vector form $Z^0 \leftarrow \begin{pmatrix} v^0 \\ w^0 \end{pmatrix}$

  Set $z(t_0) \leftarrow Z^0$

  Compute norm: $\|K\| \leftarrow \sqrt{hK^\top K}$

for $i = 0$ to $M - 1$ **do**

  Update state with (63) and control $q^{i+1} = hK^T z(t_i)$:

$$Z^{i+1} \leftarrow (I + \delta t \mathcal{A}_h)^{-1} \left(Z^i + \delta t \mathcal{B}_h z(t_i) \right)$$

  Set $z(t) \leftarrow Z^{i+1}$

  Compute difference: $d(t) \leftarrow hK^T(z(t_i) - z(t))$

  Split the vectors in components: $\begin{pmatrix} v(t) \\ w(t) \end{pmatrix} \leftarrow z(t)$, $\begin{pmatrix} v(t_i) \\ w(t_i) \end{pmatrix} \leftarrow z(t_i)$

  Compute norms: $\|v(t)\| \leftarrow \sqrt{hv(t)^\top v(t)}$ (similarly for variables $w(t)$, $v(t_i)$, $w(t_i)$)

  Compute triggering threshold:

$$\text{quotient} \leftarrow \beta \|K\| \Big(\|v(t)\|_{L^2} + \|w(t)\|_{L^2} + \|v(t_i)\|_{L^2} + \|w(t_i)\|_{L^2} \Big)$$

  if $|d| >$ quotient **then**

    Update variable: $z(t_{i+1}) \leftarrow Z^{i+1}$

  else

    Keep variable: $z(t_{i+1}) \leftarrow z(t_i)$

  end if

end for

Output: Final controlled solution $Z = (Z^n)_{n \in [\![0, M]\!]}$ and event-triggered control $q = (q^n)_{n \in [\![1, M]\!]}$.

Using such algorithm, along with the system parameters specified in (69) and (70), we aim to stabilize the free dynamics via event-triggered control. In this context, let $\epsilon = 0.1$, then the parameter β in Theorem 4.8 must be carefully selected following Remark 4.10.

Recall that we have fixed $\lambda = 4$ and $\delta = 1$, then a quick computation shows that $\vartheta = 12.154$ according to (38), $\|\Pi^{-1}\|_{L^2 \mapsto L^2} = 2.437$ and $\|k(1)\|_{L^2} = 9.744$ if $\lambda = 4$, so choosing $\beta = 0.001$ ensures (49). In Figure 4, we illustrate the time evolution of the system under event-triggered control. Notably, the small magnitude of β leads to frequent triggering, resulting in a control strategy that closely resembles continuous control (compare Figure 4c and Figure 2c). However, upon closer inspection, we can observe distinct triggers, with the control remaining constant over certain time intervals. Also, the similitude in

the control translates into a nearly indistinguishable behavior in the system's states.

To explore the effect of a less frequent triggering mechanism, we repeat the experiment with a larger value of ϵ. Keeping the same system parameters and $\lambda = 4$, we compute ϑ for $\epsilon = 0.5$, which still guarantees an exponential decay rate for the closed-loop system. In this case, we obtain $\vartheta = 4.149$, leading to a choice of $\beta = 0.005$. The corresponding figures (Figure 5) illustrate the control behavior and the system's closed-loop response under this setting.

5.4. The choice of β and its effect on the dwell-times

In Theorem 4.3, we proved the existence of a minimal (uniform) dwell-time for controlling the FHN equation with an event-triggered strategy. However, a closer examination of the proof reveals that this dwell-time is closely tied to the choice of β, which, as pointed out in Remark 4.10, depends on ϵ.

To investigate the effect of β on the dwell-time, we repeat the experiments from Section 5.3 using event-triggered controls, keeping the same parameters, but applying a much finer time mesh. In this case, we set $\delta t = 5 \times 10^{-6}$. Figure 6 shows the distribution of triggers over the time interval $[0, 4]$ for different values of β. The results indicate that, at the beginning of the interval, the density of triggers increases as β decreases, whereas in the later part of the interval, the triggers appear to be more regularly spaced.

For a more precise understanding of the relationship between β, the dwell-time, and the number of triggers, we refer to Table 1. The table presents numerical values for both the dwell-time and the exact number of triggers associated with each value of β. As β decreases, both the dwell-time and the number of triggers show opposite trends: the dwell-time decreases while the number of triggers increases. Specifically, for $\beta = 0.005$, the dwell-time is 6×10^{-5} (12 times the time step δt) with 121 triggers, while for $\beta = 0.0005$, the dwell-time drops to 1.0×10^{-5} (twice the time step δt) with 646 triggers. This illustrates that smaller values of β lead to more frequent control updates, thereby increasing the computational effort required by the system.

ϵ	β	Dwell-time	Number of triggers
0.5	0.005	6×10^{-5}	121
0.25	0.003	3.5×10^{-5}	263
0.1	0.001	1.5×10^{-5}	431
0.025	0.0005	1.0×10^{-5}	646

Table 1: Comparison of dwell-time and number of triggers for different values of β.

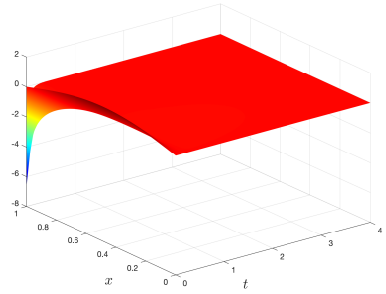

(a) The PDE component $(t, x) \mapsto v(t, x)$.

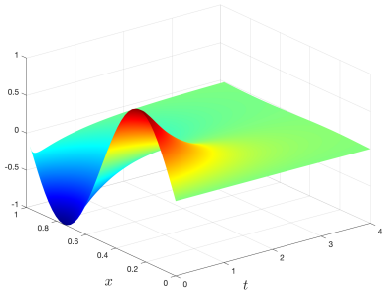

(b) The ODE component $(t, x) \mapsto w(t, x)$.

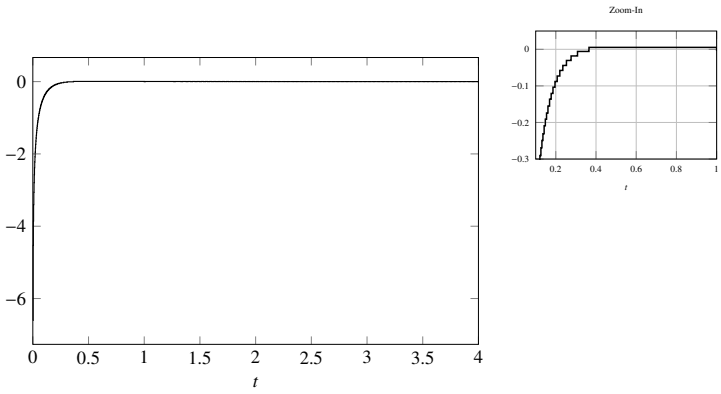

(c) Event-triggered control and zoom-in.

Figure 4: Evolution in time of the controlled system (61) with event-triggered control with design parameter $\beta = 0.001$.

Acknowledgements

Luz de Teresa is grateful to Lucie Baudouin for introducing her to the event-triggering strategies and their applications in the control of PDEs. The authors would also like to thank the anonymous referees for their valuable comments and suggestions, which have greatly improved the paper.

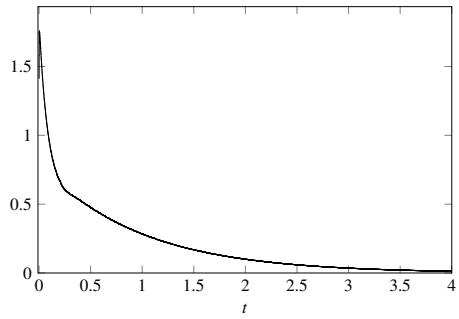

(a) Norm of the closed-loop dynamics $t \mapsto \|v(t)\|_{L^2} + \|w(t)\|_{L^2}$.

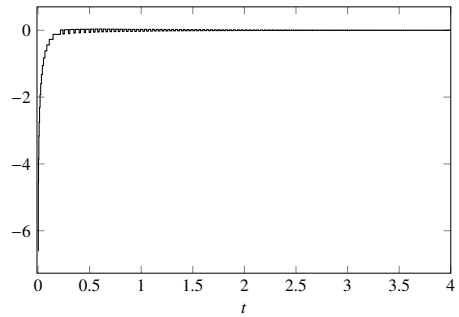

(b) Event-triggering control.

Figure 5: Evolution in time of the controlled system (61) with event-triggered control with design parameter $\beta = 0.005$.

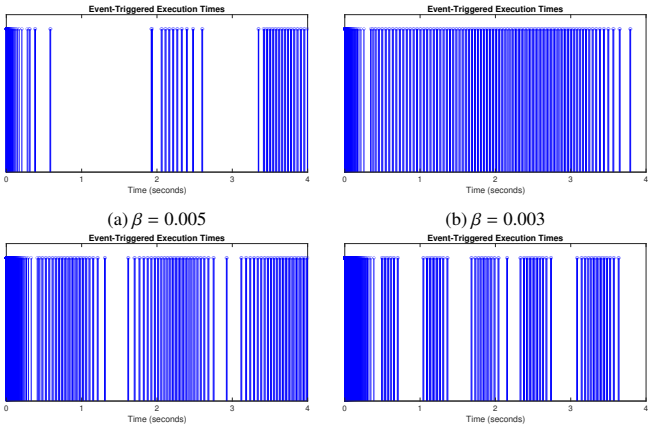

(a) $\beta = 0.005$ (b) $\beta = 0.003$

(c) $\beta = 0.001$ (d) $\beta = 0.0005$

Figure 6: Distribution of trigger events over the time interval $[0, 4]$ for different values of β. Each vertical line represents a trigger in time.

References

[1] J. Auriol. Output-feedback stabilization of an underactuated network of n interconnected $n + m$ hyperbolic pde systems. *IEEE Transactions on Automatic Control*, pages 1–12, 2024.

[2] J. Auriol and N. Espitia. Event-triggered gain scheduling of $2\times$ 2 hyperbolic pdes with time and space varying coupling coefficients. In *IEEE Conference on Decision and Control*, 2024.

[3] L. Baudouin, S. Marx, S. Tarbouriech, and J. Valein. Event-triggered boundary damping of a linear wave equation. *arXiv preprint arXiv:2303.00381*, 2023.

[4] S. Chowdhury, R. Dutta, and S. Majumdar. Boundary stabilizability of the linearized compressible Navier-Stokes system in one dimension by backstepping approach. *SIAM J. Control Optim.*, 59(3):2147–2173, 2021.

[5] S. Chowdhury, R. Dutta, and S. Majumdar. Local exponential stabilization of rogers–mcculloch and fitzhugh–nagumo equations by the method of backstepping. *ESAIM: Control, Optimisation and Calculus of Variations*, 30:41, 2024.

[6] S. Chowdhury, M. Ramaswamy, and J.-P. Raymond. Controllability and stabilizability of the linearized compressible Navier-Stokes system in one dimension. *SIAM J. Control Optim.*, 50(5):2959–2987, 2012.

[7] J.-M. Coron, A. Hayat, S. Xiang, and C. Zhang. Stabilization of the linearized water tank system. *Arch. Ration. Mech. Anal.*, 244(3):1019–1097, 2022.

[8] J.-M. Coron and H.-M. Nguyen. Null controllability and finite time stabilization for the heat equations with variable coefficients in space in one dimension via backstepping approach. *Arch. Ration. Mech. Anal.*, 225(3):993–1023, 2017.

[9] G. A. de Andrade, R. Vazquez, I. Karafyllis, and M. Krstic. Backstepping control of a hyperbolic pde system with zero characteristic speed states. *IEEE Transactions on Automatic Control*, 69(10):6988–6995, 2024.

[10] C. Demir, M. Diagne, and M. Krstic. Periodic event-triggered boundary control of neuron growth with actuation at soma. *arXiv preprint arXiv:2404.19206*, 2024.

[11] C. Demir, S. Koga, and M. Krstic. Event-triggered control of neuron growth with actuation at soma. In *2024 American Control Conference (ACC)*, pages 5301–5306. IEEE, 2024.

[12] N. Espitia. Observer-based event-triggered boundary control of a linear 2×2 hyperbolic systems. *Systems Control Lett.*, 138:104668, 10, 2020.

[13] N. Espitia, J. Auriol, H. Yu, and M. Krstic. Traffic flow control on cascaded roads by event-triggered output feedback. *Internat. J. Robust Nonlinear Control*, 32(10):5919–5949, 2022.

[14] N. Espitia, A. Girard, N. Marchand, and C. Prieur. Event-based control of linear hyperbolic systems of conservation laws. *Automatica J. IFAC*, 70:275–287, 2016.

[15] N. Espitia, A. Girard, N. Marchand, and C. Prieur. Event-based boundary control of a linear 2×2 hyperbolic system via backstepping approach. *IEEE Trans. Automat. Control*, 63(8):2686–2693, 2018.

[16] N. Espitia, I. Karafyllis, and M. Krstic. Event-triggered boundary control of constant-parameter reaction-diffusion PDEs: a small-gain approach. *Automatica J. IFAC*, 128:Paper No. 109562, 10, 2021.

[17] L. Gagnon, P. Lissy, and S. Marx. A Fredholm transformation for the rapid stabilization of a degenerate parabolic equation. *SIAM J. Control Optim.*, 59(5):3828–3859, 2021.

[18] S. P. Hastings. Some mathematical problems from neurobiology. *Amer. Math. Monthly*, 82(9):881–895, 1975.

[19] A. Hayat and E. Loko. Fredholm backstepping and rapid stabilization of general linear systems. HAL preprint, June 2024.

[20] W. Heemels, K. Johansson, and P. Tabuada. An introduction to event-triggered and self-triggered control. *Proceedings of the IEEE*, 100(1):60–78, 2012.

[21] W. Kang, L. Baudouin, and E. Fridman. Event-triggered control of Korteweg–de Vries equation under averaged measurements. *Automatica J. IFAC*, 123:Paper No. 109315, 11, 2021.

[22] I. Karafyllis, N. Espitia, and M. Krstic. Event-triggered gain scheduling of reaction-diffusion PDEs. *SIAM J. Control Optim.*, 59(3):2047–2067, 2021.

[23] I. Karafyllis and M. Krstic. Sampled-data boundary feedback control of 1-D parabolic PDEs. *Automatica J. IFAC*, 87:226–237, 2018.

[24] R. Katz, E. Fridman, and A. Selivanov. Network-based boundary observer-controller design for 1d heat equation. In *2019 IEEE 58th Conference on Decision and Control (CDC)*, pages 2151–2156. IEEE, 2019.

[25] R. Katz, E. Fridman, and A. Selivanov. Boundary delayed observer-controller design for reaction-diffusion systems. *IEEE Trans. Automat. Control*, 66(1):275–282, 2021.

[26] F. Koudohode, L. Baudouin, and S. Tarbouriech. Event-based control of a damped linear schrödinger equation. In *2022 European Control Conference (ECC)*, pages 2099–2104, 2022.

[27] F. Koudohode, L. Baudouin, and S. Tarbouriech. Event-based control of a damped linear wave equation. *Automatica*, 146:110627, 2022.

[28] F. Koudohode, N. Espitia, and M. Krstic. Event-triggered boundary control of an unstable reaction diffusion PDE with input delay. *Systems Control Lett.*, 186:Paper No. 105775, 9, 2024.

[29] M. Krstic and A. Smyshlyaev. *Boundary control of PDEs*, volume 16 of *Advances in Design and Control*. Society for Industrial and Applied Mathematics (SIAM), Philadelphia, PA, 2008. A course on backstepping designs.

[30] K. Kunisch and D. A. Souza. On the one-dimensional nonlinear monodomain equations with moving controls. *J. Math. Pures Appl. (9)*, 117:94–122, 2018.

[31] P. Lissy and C. Moreno. Rapid stabilization of a degenerate parabolic equation using a backstepping approach: the case of a boundary control acting at the degeneracy. *Math. Control Relat. Fields*, 14(3):1007–1032, 2024.

[32] W. Liu. Boundary feedback stabilization of an unstable heat equation. *SIAM J. Control Optim.*, 42(3):1033–1043, 2003.

[33] W. Liu. *Elementary feedback stabilization of the linear reaction-convection-diffusion equation and the wave equation*, volume 66 of *Mathématiques & Applications (Berlin) [Mathematics & Applications]*. Springer-Verlag, Berlin, 2010.

[34] H. Parada and G. Arias. Boundary stabilization of a class of coupled reaction-diffusion system with one control. HAL preprint, Apr. 2024.

[35] R. Plonsey, R. C. Barr, and F. X. Witkowski. One-dimensional model of cardiac defibrillation. *Medical and Biological Engineering and Computing*, 29(5):465–469, 1991.

[36] R. Postoyan, P. Tabuada, D. Nešić, and A. Anta. Framework for event-triggered and self-triggered control. *IEEE Transactions on Automatic Control*, 60(10):2644–2659, 2014.

[37] B. Rathnayake and M. Diagne. Observer-based event-triggered boundary control of the one-phase stefan problem. *International Journal of Control*, pages 1–12, 2024.

[38] B. Rathnayake and M. Diagne. Observer-based periodic event-triggered and self-triggered boundary control of a class of parabolic pdes. *IEEE Transactions on Automatic Control*, pages 1–8, 2024.

[39] B. Rathnayake, M. Diagne, J. Cortés, and M. Krstic. Performance-barrier event-triggered control of a class of reaction–diffusion PDEs. *Automatica J. IFAC*, 174:Paper No. 112181, 2025.

[40] B. Rathnayake, M. Diagne, N. Espitia, and I. Karafyllis. Observer-based event-triggered boundary control of a class of reaction-diffusion PDEs. *IEEE Trans. Automat. Control*, 67(6):2905–2917, 2022.

[41] J. Rogers and A. McCulloch. A collocation-galerkin finite element model of cardiac action potential propagation. *IEEE Transactions on Biomedical Engineering*, 41(8):743–757, 1994.

[42] A. Selivanov and E. Fridman. Distributed event-triggered control of diffusion semilinear PDEs. *Automatica J. IFAC*, 68:344–351, 2016.

[43] E. Somathilake, B. Rathnayake, and M. Diagne. Output feedback periodic event-triggered control of coupled 2× 2 linear hyperbolic pdes. *arXiv preprint arXiv:2404.02298*, 2024.

[44] T. Strecker, M. Cantoni, and O. M. Aamo. Event-triggered boundary control of semilinear hyperbolic systems. *IEEE Transactions on Automatic Control*, 69(1):418–425, 2023.

[45] P. Tabuada. Event-triggered real-time scheduling of stabilizing control tasks. *IEEE Transactions on Automatic Control*, 52(9):1680–1685, 2007.

[46] R. Vazquez, J. Auriol, F. Bribiesca-Argomedo, and M. Krstic. Backstepping for partial differential equations. *arXiv preprint arXiv:2410.15146*, 2024.

[47] J. Wang and M. Krstic. Adaptive event-triggered PDE control for load-moving cable systems. *Automatica J. IFAC*, 129:Paper No. 109637, 14, 2021.

[48] J. Wang and M. Krstic. Event-triggered output-feedback backstepping control of sandwich hyperbolic PDE systems. *IEEE Trans. Automat. Control*, 67(1):220–235, 2022.

[49] J. Wang and M. Krstic. Event-triggered adaptive control of a parabolic PDE-ODE cascade with piecewise-constant inputs and identification. *IEEE Trans. Automat. Control*, 68(9):5493–5508, 2023.

[50] P. Zhang, B. Rathnayake, M. Diagne, and M. Krstic. Performance-barrier event-triggered pde control of traffic flow. *arXiv preprint arXiv:2501.00722*, 2025.